

Conventional sub-soil irrigation techniques do not lower greenhouse gas carbon emission from drained peat meadows

Stefan Theodorus Johannes Weideveld^{1*}, Weier Liu², Merit van den Berg¹, Leon Peter Maria Lamers¹,
5 Christian Fritz¹,

¹ - Aquatic Ecology and Environmental Biology, Institute for Water and Wetland Research, Radboud University, Heyendaalseweg 135, 6525, AJ, Nijmegen, the Netherlands.

² - Integrated Research on Energy, Environment and Society, University of Groningen, Nijenborgh 6, 9747 AG, Groningen,
10 the Netherlands

**Corresponding author*

E-mail addresses: Stefan.Weideveld1@gmail.com, S.Weideveld@science.ru.nl (S.T.J. Weideveld)

Abstract

The focus of current water management in drained peatlands is to facilitate agricultural use optimal drainage, which has, leads to soil subsidence and strongly increases increased of greenhouse gas (GHG) emission. High density, The Dutch land and water authorities proposed the application of sub-soil irrigation (SSI) systems on a large scale in high density have been proposed to potentially reduce GHG emissions as a potential climate mitigation measure, while maintaining high biomass production. In summer, SSI was Based on model results. They the expectedation was that SSI would to reduce peat decomposition in summer by preventing groundwater tables (GWT) to drop below -60 cm. In 2017–2018, we evaluated the effects of SSI on GHG emissions (CO₂, CH₄, N₂O) for four dairy farms on drained peat meadows in the Netherlands. Each farm had a treatment site with SSI installation and a control site drained only by ditches (ditch water level -60/-90 cm, 100 m distance between ditches). The SSI system consisted of perforated pipes at 70 cm below ground surface soil level with spacing of 5–6 m to improve both drainage during (winter–spring) and irrigation in (summer) of the subsoil, and a control site drained only by ditches (ditch water level -60/-90 cm, 100 m distance between ditches). GHG emissions were measured using closed

25 chambers (0.8 \times 0.8 m) every 2–4 weeks for CO₂ and CH₄ and N₂O. C inputs by manure and C export by grass yields were accounted for. Unexpectedly, SSI hardly affected ecosystem respiration (R_{eco}) despite raising summer groundwater tables (GWT) by 6–18 cm, and even up to 50 cm during drought. Only Measured ecosystem respiration (R_{eco}) did not show significant difference between SSI and control sites only except only showed a small difference between SSI and control sites when the groundwater table (GWT) of SSI sites was were substantially higher than the control site value (> 20 cm difference). Over all 30 years and locations, however, there was no significant difference found, despite the 6–18 cm higher GWT in summer and 1–20 cm lower GWT in wet conditions at SSI sites—on average in the four farm locations. Differences in mean annual GWT remained low (< 5 cm). Direct comparison of measured N₂O and CH₄ fluxes between SSI and control sites did not show any significant differences. CO₂ fluxes varied according to temperature and management events while differences between control and SSI sites remained small. R_{eco} was significantly lower ($p < 0.01$), indicating a small effect of irrigation on C turnover.

35 During wet conditions sub-soil pipes lowered water levels by 1–20 cm, without a significant effect on R_{eco}. As a result, R_{eco} differed little (>3%) between SSI and control sites on an annual base. CO₂ fluxes were high at all locations, ranging from 35–66 and 20–50 t CO₂ ha⁻¹ yr⁻¹ in 2017 and 2018, respectively, even where peat was covered by clay (25–40 cm). Despite extended drought episodes and lower water levels in 2018, we found lower annual CO₂ fluxes than in 2017 indicating drought stress for microbial respiration. Contrary to our expectation, Overall Therefore, there was no difference between the annual 40 CO₂ fluxes gap-filled net ecosystem exchange (NEE) GHG fluxes of the sub-soil irrigated SSI and control site. The net ecosystem carbon balance was on average (40 and 30 t CO₂ eq ha⁻¹ yr⁻¹ in 2017 and 2018 on the SSI sites) and control sites (38 and 34 t CO₂ eq ha⁻¹ yr⁻¹ in 2017 and 2018 on the control sites). SSI did not affect average N₂O emissions, although the number of flux measurements were limited to draw strong conclusions about the treatment effects.

Emissions of N₂O were lower with average emissions were measured ($2.9 \pm 1.8 \text{ mg N}_2\text{O} \cdot \text{m}^{-2} \cdot \text{d}^{-1}$ for 2017) in 2017 than in 2018 45 (3.6 \pm 3.3 mg N₂O · m⁻² · d⁻¹), without treatment effects. No SSI effect was detected for CH₄. The contribution of CH₄ to the total GHG budget was negligible (<0.1%), with lower GWT favoring CH₄ oxidation over its production. Moreover, NEE was summed up with C inputs by manure and C export by grass yield into net ecosystem carbon balance (NECB), whereas No 50 treatment effect was found on yields, suggesting that the increased GWT in summer did not increase plant water supply. This lack of SSI effect is probably because the GWT increase remains limited to s only takes place in deeper soil layers (60–120

50 cm depth), which ~~also indicates that could hardly affect contribute contribute little to~~ peat oxidation ~~is hardly affected and plant water supply.~~

We conclude that ~~although our field scale experimental research revealed substantial differences in summer GWT and timing/intensity of irrigation and drainage, SSI modulates water table dynamics but~~ fails to lower annual GHG carbon emission. ~~SSI and is seems~~ unsuitable as a climate mitigation strategy. Future research should focus on potential effects of
55 GWT manipulation in the uppermost organic layers (-30 cm and higher) on GHG emissions from drained peatlands.

1 Introduction

Peatlands cover only 3% of the land and freshwater surface of the planet, yet they contain one third of the total carbon (C) stored in soils (Joosten and Clarke, 2002). Natural peatlands capture C by producing more organic material than ~~is~~decomposed due to waterlogged conditions (Gorham et al., 2012;Lamers et al., 2015). Drainage of peatlands for agricultural purposes leads
60 to aerobic oxidation of organic material ~~and increased gas exchange resulting in soil subsidence and the concomitant release~~releasing ~~of~~ CO₂ and N₂O ~~at high rates~~ (Regina et al., 2004;Joosten, 2009;Hoogland et al., 2012;Lamers et al., 2015;Leifeld and Menichetti, 2018). Soil subsidence occurs when the groundwater table (GWT) drops through drainage, leading to physical and chemical changes of the peat ~~including microbial breakdown of organic matter~~. This results in consolidation, shrinkage, compaction and increased decomposition (Stephens et al., 1984;Hooijer et al., 2010). Soil subsidence
65 increases the risk of flooding (frequency and duration) in areas where soil surface subsides below river and sea levels (Svitski et al., 2009). In the Netherlands, 26% of the surface area is currently below sea level, an area currently inhabited by 4 million people (Kabat et al., 2009). This area is expected to increase due to further land subsidence, while sea level is rising at the same time, which is a general issue of coastal peatlands (Erkens et al., 2016;Herrera-García et al., 2021). Additionally, peatland subsidence alters hydrology ~~on various scales, which~~ leading to ~~frequent~~ drainage ~~failure problems~~ difficulties, salt
70 ~~water~~saltwater intrusion and loss of productive lands (Dawson et al., 2010;Herbert et al., 2015). ~~This will result in strongly Ongoing peatland subsidence increased inflict high~~ societal costs and difficulties in maintaining productive land use (Van den Born et al., 2016;Tiggeloven et al., 2020).

75 The peatland area used for agriculture is estimated at 10% for the USA and 15% for Canada, and varies from less than 5 to more than 80% ~~or in European countries~~ (Lamers et al., 2015). In the Netherlands, 85% of the peatland areas are in agricultural use (Tanneberger et al., 2017), leading to CO₂ emissions of 7 Mt CO₂-eq per year, ~~amounting accounting for >25% of total to 4% of total national~~ greenhouse gas (GHG) emissions from Dutch agriculture (Arts et al., 2020). Fundamental changes in the management of peatlands are required if land use, biodiversity and socio-economic values including GHG emission reduction
80 are to be maintained.

~~Carbon dioxide~~CO₂ emissions from peatlands are related to the ~~water table position~~GWT position below surface, which affects oxygen intrusion, moisture content and temperature. There is ample evidence that elevating ~~water levels~~GWT to 0-20 cm below ~~the land~~ surface results in substantial reduction of CO₂ emissions from (formerly) managed peatlands (Hendriks et al.,
85 Hiraishi et al., 2014; Jurasinski et al., 2016; Tiemeyer et al., 2020). Increasing ~~water levels~~GWT close to the surface does not only ~~worsens conditions for constraints~~ aerobic CO₂ production and rapid gas exchange but also reduces land-use intensity (fertilization, tillage, planting, grazing). Additionally, high ~~water levels~~GWT could favor vegetation assemblages with a higher carbon sequestration potential (e.g. peat forming plants) compared to common fodder grasses and crops. Experimental ~~research~~
~~using studies on~~ water table manipulations ~~stressed~~ the importance of rewetting the upper 20-30 cm to achieve noteworthy
90 CO₂ emissions reduction (Regina, 2014; Karki et al., 2016) which seems in line with the correlation of CO₂ emissions with GWT based on a meta-analysis of field CO₂ emission data by Tiemeyer et al. (2020).

Dutch water- and land-authorities have relied on ~~height-ground surface elevation~~ measurements to estimate peat loss of the peat
95 ~~surface~~ rather than CO₂ flux measurements to estimate come to calculate CO₂ emissions from peatlands (Arts et al., 2020) and the effects of elevated ~~water levels~~GWT on CO₂ emissions. Two assumptions are generally made when inferring ~~translating~~ surface elevation data into CO₂ emission from surface elevation changes: 1) -Elevation changes are directly related to C losses from peatlands within a time frame of years ignoring physical changes of peat following drainage. As a conversion factor 2.23

t CO₂ ha⁻¹ per mm subsidence is assumed (Kuikman et al., 2005;Van den Akker et al., 2010). 2) The average lowest summer

100 GWT (GLG) is assumed to be a major control factor of subsidence rates of peat surface elevation and henceforth CO₂ emissions based on the first assumption above (Arets et al., 2020). As a consequence of both assumptions, Dutch climate mitigation frameworks focus on elevating summer GWT in peatlands rather than mean annual GWT (Querner et al., 2012;Brouns et al., 2015). Dutch water- and land-authorities expect that increasing the average lowest summer GWT by 20 cm would result in an emission reduction equalling 10.5 t CO₂ ha⁻¹ yr⁻¹ (Van den Akker et al., 2007;Brouns et al., 2015;Van den Born et al., 2016).

105

The use of subsoil irrigation and drainage systems (SSI)~~SSI systems has have~~ been proposed to elevate summertime GWT

and thereby presumably reducing CO₂ emissions since the early 2000's (Van den Akker et al., 2010;Querner et al., 2012). SSI

110 works by installing perforated drainage/irrigation pipes at around 70 cm below the surface and or at least 10 cm below the

ditch water level. Water from the ditch can infiltrate into the adjacent peat adjacent to drainageSSI pipes and thereby limite

115 GWT drawdowns during summer (c.f. (Hoving et al., 2013). Next to irrigation, drainageSSI pipes primarily fulfill a drainage

function when the GWT is above the ditch water level. Based on the elevating effects on summer groundwater table SSI was

assumed to reduce of C emissions from peatlands by 50% according to the soil-carbon-water model (Querner et al., 2012;Van

120 den Born et al., 2016). However, th effect of SSI on C emissions has nog yet been tested by field measurements of C-fluxes.

based on the soil carbon water model assumptions that peat layers below 70 cm contribute largely to GHG emissions and that

surface elevation differences can be translated directly into CO₂ emission

The aim of our study was to quantify the effects of SSI on the GWT and GHG emissions, in particular with consideration of

125 the farm field net ecosystem carbon balance (NECB). We questioned 1) to what extent can SSI regulate GWT, especially

during dry conditions in summer, 2) whether the SSI can substantially reduce (up to 50% as assumed by authorities) CO₂

emission compared to traditional ditch drainage.~~—, and 3) whether nitrous oxide peaks are lowered by SSI~~ To adress these

questions we directly compared GHG emissions from a control grassland (traditional ditch drainage) with a treatment grassland

(SSI) on four farms over a periode of 2 years.

125 **2 Material and methods****2.1 Study area**

The study areas are located in a peat meadow area in the province of Friesland, the Netherlands. The climate is humid Atlantic with an average annual precipitation of 840 mm and an average annual temperature of 10.1 °C (KNMI, reference period 1999-2018).

130 About 62% of the Frisian peatland region is now used as grassland for dairy farming (Hartman et al., 2012). Agricultural land in Friesland is farmed intensively, with high yields, and intensive fertilization ($>230 \text{ kg N ha}^{-1} \text{ yr}^{-1}$). ~~It is characterized by combined with large-wide fields with deep drainage.~~ ~~One third of the fields are drained to -90 – -120 cm below soil surface. Large parts of these grasslands are covered with a carbon rich clay layer, ranging from 20–40 cm thick. The peat layer below has a thickness of 80–200 cm, which consists of sphagnum peat on top of sedge, reed and alder peat. The top 30 cm of~~
 135 ~~the peat layer is strongly humified (van Post H8-H10) and the peat below 60 – 70 cm deep is only moderately decomposed (van Post H5-H7). On two locations (C and D, see below), there is a ‘schalter’ peat layer present, which is highly laminated peat (compacted/ hydrophobic layers of *Sphagnum cuspidatum* remnants) with poor degradability and poor water permeability.~~
 The grasslands ~~are-were~~ dominated by *Lolium perenne*; other species such as *Holcus lanatus*, *Elytrigia repens*,
~~Ranunculus acris~~ and *Trifolium repens* ~~are-were~~ present in a low abundance in 2017-2019.

140

Table 1 Soil and land-use characteristics of the research sites in the peat meadows of Friesland, the Netherlands.* ~~Displayed concentrations of the top 70 cm. Averages per soil type, gravimetric soil moisture content taken August 2017, Dry bulk density, Organic matter content, and elemental Carbon content.~~

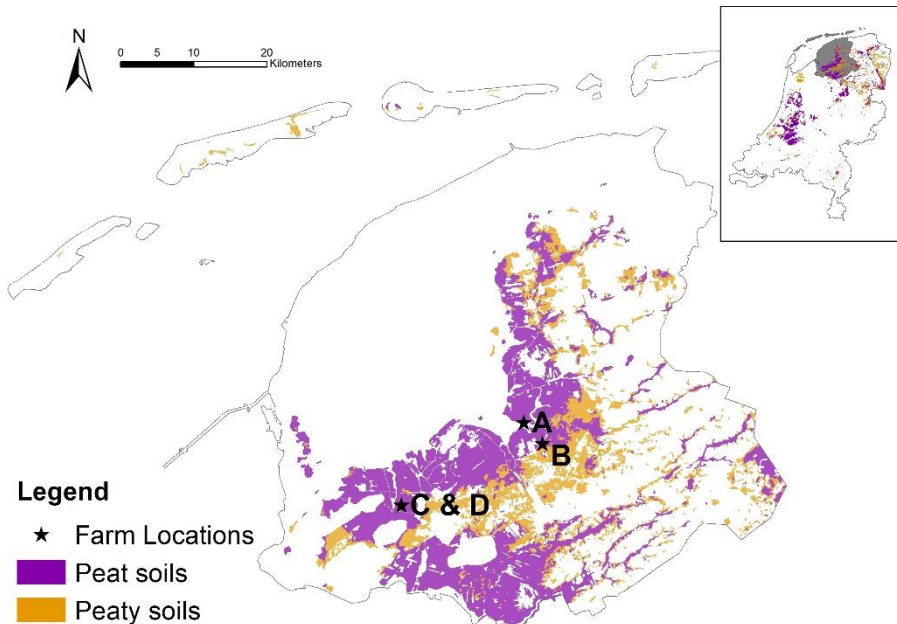
Location	Farm type	management	Treatment	mineral				Organic matter g/4	Carbon content kg C m ⁻² 70cm	C:N*
				Field size ha	top layer thickness m	schalter present	thickness peat layer m			
A	Organic	Grazing	SSI	2	0.35	-	1.6	132.9	53.4	29.2
-	-	-	Control	0.6	0.40	-	2.0	141.2	47	19.8
B	Conventional	Grazing	SSI	2.3	-	-	1.4	190.7	68.1	34.6
-	-	-	Control	2.3	-	-	1.4	175.9	74.9	32.8
C	Conventional	Mowing	SSI	1.2	0.30	yes	1.3	141.7	56.3	23

-	-	-	Control	1.8	0.30	yes	1.0	133.4	60.5	23.5
D	Conventional	Mowing	SSI	2.4	0.30	yes	0.9	161.9	59.6	23.3
-	-	-	Control	3.5	0.25	yes	0.9	151.5	63.4	26.9

Farm	Treatment	Field size	peat thickness	Soil type	Soil depth	Soil moisture	Bulk density	Organic matter	Carbon content	Carbon content
		ha	m		cm	%	g DW/cm ³	g Org/L	g C/l	g C/kg
A)	SSI	2 ha	1.6 m	Mineral	0 – 35	38.1	0.99	123	52	53
Organic				Peat	35 – 60	77.1	0.23	144	77	335
Grazing				Peat	60 – 80	82.1	0.14	130	68	485
	Control	0.6 ha	2 m	Mineral	0 – 40	37.6	0.93	130	54	58
				Peat	40 – 60	59.2	0.24	156	83	345
				Peat	60 – 80	85.3	0.16	154	98	613
B)	SSI	2.3 ha	1.4 m	Peat	0 – 20	51	0.44	270	108	245
Conventional				Peat	20 – 60	79.3	0.19	169	77	403
Grazing				Peat	60 – 80	88.4	0.12	118	60	499
	Control	2.3 ha	1.4 m	Peat	0 – 20	50.1	0.49	273	138	282
				Peat	20 – 60	77.7	0.17	141	72	424
				Peat	60 – 80	86.5	0.13	122	67	515
C	SSI	1.2 ha	1.3 m	Mineral	0 – 30	36	0.71	128	58	82
Conventional				Schalter	30 – 40	79.2	0.19	177	88	461
Mowing				Peat	40 – 60	82.2	0.18	129	64	357
				Peat	60 – 80	87.5	0.11	133	81	740
	Control	1.8 ha	1 m	Mineral	0 – 30	38	0.75	142	59	79
				Schalter	30 – 40	78.7	0.19	177	92	486
				Peat	40 – 60	84.3	0.12	116	60	499
				Peat	60 – 80	89.2	0.1	134	72	715
D	SSI	2.4 ha	0.9 m	Mineral	0 – 30	37.7	0.85	155	74	87
Conventional				Schalter	30 – 40	63.9	0.3	267	85	284
Mowing				Peat	40 – 60	84.3	0.19	137	73	385
	Control	3.5 ha	0.9 m	Mineral	0 – 25	32.9	0.82	141	73	89

Schalter	<u>25 – 35</u>	<u>70</u>	<u>0.27</u>	<u>173</u>	<u>86</u>	<u>318</u>
Peat	<u>35 – 60</u>	<u>84.1</u>	<u>0.15</u>	<u>142</u>	<u>83</u>	<u>551</u>
Peat	<u>60 – 80</u>	<u>81.9</u>	<u>0.11</u>	<u>109</u>	<u>70</u>	<u>632</u>

145



150

Figure 1 Soil map with field locations situated in the province of Friesland, of the Netherlands, with soil types. Peat soils refer to soils with an organic layer of at least 40 cm within the first 120 cm, while peaty soils are soils with an organic layer of 5-40 cm within the first 80 cm. Insert shows these soil types in the Netherlands, with the location of the field locations in grey.

2.2 Experiment setup

155

Four sites were set up at dairy farms with land management and soil types representative for Friesland (see Table 1 and Fig. 1). Each location consisted of a treatment site with SSI pipes and a control site. The irrigation-SSI pipes were installed at a depth of 70 cm below the surface and 5–6 m (2,000 m drains ha⁻¹) apart from each other, except for the D location where pipes were 5 m apart. The overall drainage intensity was around 2000 m ha⁻¹. The pipes were either directly connected to the ditch (A and C) or connected to a collection-collector tube before connected into the that was connected to a ditch (B and D). The connections with ditches were placed 10 cm below the maintained-targeted ditchwater level that was regulated by a

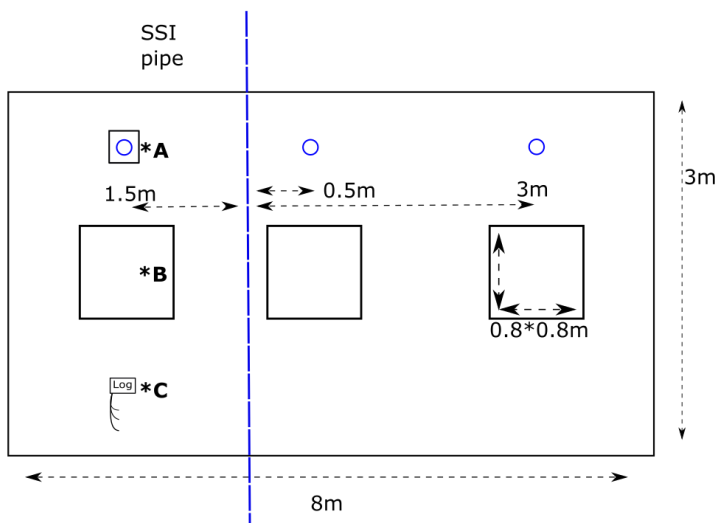
complex network of water inlet and pumps at the lowest parts of the polder. The control sites are fields that have traditional drainage, ~~through a system~~ with deep drainage ditches with convex fields and small shallow ditches (furrows).

165 On the treatment sites, three gas measurement frames ~~in 80x80~~ ~~80 × 80~~ cm ~~squares~~ were placed for the duration of the experiment on 0.5 m, 1.5 m and 3 m distance from the chosen ~~irrigation-SSI~~ pipe (Fig. 2), representing best the variation in the environmental conditions and vegetation. The control sites where located 32 – 42 m from the ditch. Dip well tubes were installed to monitor water ~~leveltables~~ 0.5, 1.5 and 3 m from the pipe, pairing with the locations of gas measurement frames (Fig. 2). The nylon coated tubes were 5 cm wide and perforated filters (130-150 cm length) were placed in the peat layer. The 170 tube 1.5 m from the ~~irrigationSSI~~ pipe was equipped with a pressure sensor and a data logger (ElliTrack-D, Leiderdorp instruments, Leiderdorp, Netherlands) that measures and records the GWT every hour. Ten more dip well tubes were further placed at intervals 0.5 and 3 m from the pipes in the field, which were manually sampled every 2 weeks during gas sampling campaigns, to obtain the variation on field scale.

175 To determine soil properties, \$soil samples were taken using a gouge auger ~~in three replicates~~ ~~till ...0.8 m depth where taken, from~~ 1.5 meter from the ~~irrigation-SSI~~ pipes every... moment in year taken in august 20172. To determine moisture content, \$For soil moisture, ~~s~~ediment samples were weighed and subsequently oven-dried at 105°C for 24 h. Organic matter content was determined via loss- on ignition. Dried sediment samples ~~were~~ incinerated ~~for~~ 4 h at 550°C (Heiri et al., 2001). Total nitrogen (TN) and total carbon (TC) was determined in soil material (9~~–~~23 mg) using an elemental CNS analyzer (NA 1500, 180 Carlo Erba; Thermo Fisher Scientific, Franklin, USA).

Soil temperature at -5, -10 and -20 cm depth ~~and soil moisture~~ were continuously measured (12-Bit Temperature sensor -S-TMB-M002 ~~and 10HS Soil Moisture Smart Sensor~~, Onset Computer Corporation, Bourne, USA) during the run time of the experiment and recorded every 5 ~~minutes~~ on a data logger (HOBO H21-USB Micro Station Onset Computer Corporation, 185 Bourne, USA). Because of the frequent failure of sensors, extra temperature sensors (HOBO™ pendant loggers, model UA-002-64, Onset Computer Corporation, Bourne, USA) were placed in the soil at a depth of -5 and -10 cm.

At farms A and D, sensors were set up at 1.5 m above ground to measure photosynthetically active radiation (PAR, Smart Sensor S-LIA-M003, ONSET Computer Corporation, Bourne, USA), air temperature and air relative humidity 190 (Temperature/Relative Humidity Smart Sensor, S-THB-M002, Onset Computer Corporation, Bourne, USA). Data were logged every 5 minutes (HOBO H21-USB Micro Station, Onset Computer Corporation, Bourne, USA). Average air temperature and precipitation from the weather station Leeuwarden (18 to 30 km distance from research sites) were used. (KNMI, data). The location specific precipitation was estimated using radar images with a resolution of 3 x 3 km



195

Figure 2 Overview field site SSI. Blue dashed line = irrigation SSI pipe, blue circle = dipwell, *A – dipwell with data logger, *B – gas-greenhouse gas flux measurement frame, *C – data logger, -5 -10 -20 soil temperature and soil moisture

200

C-export from frames used GHG measurements was determined by harvesting the frames the standing biomass eight times in 2017 and five times in 2018. Two extra of the harvest moments where implemented in 2017 were extra planned, once in May to because of the fast grass growth and extreme grass height exceeding 30 cm, and the other in December to come back to the in order to reset the grass height at the start of the experiment for next year. The surrounding Surrounding the frames A and an area of 8 x 3 m was fenced off field site surrounding the measurement frames to avoid disturbance from grazing and other

205 ~~field managementsactivities (Fig. 2). ThisThe fieldfenced-off area outside the frames was the whole field site were~~ managed with 4–5 cuts per year to have a similar grass height with ~~the farmland the surrounding field~~. The biomass was harvested, ~~where~~ weighed for fresh weight and dried at 70 °C until constant weight. Total nitrogen (TN) and total carbon (TC) was determined in dry plant material (3 mg) using an elemental CNS analyzer (NA 1500, Carlo Erba; Thermo Fisher Scientific, Franklin, USA). Due to grazing disturbance in 2018, an estimation instead of measurements was made for the C-export of location A in consultation with the farmer, but excluded from statistical analysis. Four times per year slurry manure from location C was applied to all plots. The slurry was diluted with ditchwater (2:1 ratio) and applied above ground in the gas measurement frames and the surrounding area. (119 – 181 kg N ha⁻¹ yr⁻¹ for 2017 and 129 – 162 kg N ha⁻¹ yr⁻¹ for 2018 with a C/N ratio of 16.3±1.3

210 **2.3 Flux measurements**

CO₂ exchange was measured from January 2017 to December 2018, at a frequency of two measurement campaigns a month during growing season (April – October) and once a month during winter. This resulted in 34 (A), 35 (C and D) and 38 (B) campaigns over the two years for CO₂ and CH₄. The N₂O emissions ~~were~~ measured with a lower frequency with 22 (A), 20 (B and C) and 17 (D) campaigns over the two years. A measurement campaign consisted of flux measurements with opaque (dark) and transparent (light) closed chambers (0.8x0.8x0.5 m) to be able to distinguish ecosystem respiration (R_{eco}) and gross primary production (GPP) from net ecosystem exchange (NEE). During winter an average of 9 light and 10 dark measurements, and during summer 18 light and 20 dark measurements were carried out over the course of the day, to achieve data over a gradient in soil temperature and PAR.

220 The chamber was placed on a frame installed into the soil and connected to a fast greenhouse gas analyzer (GGA) with cavity ring-down spectroscopy (GGA-30EP, Los Gatos Research, Santa Clara, CA, USA) to measure CO₂ and CH₄ or to a G2508 gas concentration analyzer with cavity ring-down spectroscopy (G2508 CRDS Analyzer, Picarro, Santa Clara, CA, USA) to measure N₂O. To prevent heating and to ensure thorough mixing of the air inside the chamber, the chambers ~~were~~ equipped with two fans running continuously during the measurements. For CO₂ and CH₄, each flux measurement lasted on average 180s. N₂O fluxes were measured on all frames at least once during a measurement campaign, with an opaque chamber for 480s per flux.

PAR was manually measured (Skye SKP 215 PAR Quantum Sensor, Skye instruments Ltd, Llandrindod Wells, United Kingdom) during the transparent measurements, on top of the chamber. The PAR value was corrected for transparency of the 230 chamber. Within each measurement, a variation in PAR higher than $75 \mu\text{mol m}^{-2} \text{s}^{-1}$ would lead to a restart of the measurement. Soil temperature was measured manually in the frame after the dark measurements at -5 and -10 cm depth (Greisinger GTH 175/PT Thermometer, GMH Messtechnik GmbH, Regenstauf, Germany). ~~Crop~~ ~~Grass~~ height was measured using a straight scale with a plastic disk with a diameter of 30 cm before starting the measurement campaign.

2.4 Data analyses

235 2.4.1 Flux calculations

Gas fluxes were calculated using the slope of gas concentration over time (Almeida et al., 2016) (eq.1).

$$F = \frac{V}{A} * \text{slope} * \frac{P * F1 * F2}{R * T} \quad (1)$$

Where F is gas flux ($\text{mg m}^{-2} \text{d}^{-1}$), V is chamber volume (0.32 m^3), A is the chamber surface area (0.64 m^2), slope is the gas 240 concentration change over time (ppm second^{-1}); P is atmospheric pressure (kPa); F1 is the molecular weight, 44 g mol^{-1} for CO_2 and N_2O and 16 g mol^{-1} for CH_4 ; F2 is the conversion factor of seconds to days; R is gas constant ($8.3144 \text{ J K}^{-1} \text{ mol}^{-1}$); and T is temperature in Kelvin (K) in the chamber.

2.4.2 R_{eco} modeling

To gap-fill for the days that were not measured for an annual balance for CO_2 exchange, R_{eco} and GPP models needed to be 245 fitted with the measured data for each measurement campaign. R_{eco} was fitted with the Lloyd-Taylor function (Lloyd and Taylor, 1994) based on soil temperature (Eq. 2):

$$R_{\text{eco}} = R_{\text{eco},T_{\text{ref}}} * e^{E_0 * \left(\frac{1}{T_{\text{ref}} - T_0} - \frac{1}{T - T_0} \right)} \quad (2)$$

250 ~~W~~here R_{eco} is ecosystems respiration, $R_{\text{eco},T_{\text{ref}}}$ is ecosystem respiration at the reference temperature (T_{ref}) of 281.15 K and was fitted for each measurement campaign, E_0 is long term ecosystem sensitivity coefficient (308.56, (Lloyd and Taylor,

1994)), T_0 Temperature between 0 and T (227.13, Lloyd and Taylor, 1994), T is the observed soil temperature (K) at 5 cm depth and T_{ref} is the reference temperature (283.15 K). If it was not possible to get a significant relationship between the T and the R_{eco} with data from a single campaign, data were pooled for two measuring days to achieve significant fitting (Beetz et al., 2013; Poyda et al., 2016; Karki et al., 2019)

255 **2.4.3 GPP modeling**

GPP was obtained by subtracting the measured R_{eco} (CO_2 flux measured with the dark chambers) from the measured NEE (CO_2 flux measured with the light chambers) ~~according to measurement time~~. For the days in between the measurement campaigns, data were modeled with the relationship between the GPP and PAR using a Michaelis–Menten light optimizing response curve (Beetz et al., 2013; Kandel et al., 2016). For each measurement location per measurement campaign, the GPP 260 was modeled by the parameters α and GPP_{max} (maximum photosynthetic rate with infinite PAR) of (eq.3):

$$GPP = \frac{\alpha * PAR * GPP_{max}}{GPP_{max} + \alpha * PAR} \quad (3)$$

where ~~NEE GPP~~ is the ~~measured corrected~~ CO_2 flux ~~with light chamber measured with lighttransperant chambers and corrected with R_{eco}~~, α is ecosystem quantum yield ($\text{mg CO}_2 \cdot \text{C m}^{-2} \text{ h}^{-1}$)/($\mu\text{mol m}^{-2} \text{ s}^{-1}$) which is the linear change of GPP per change in PAR at low light intensities (<400 $\mu\text{mol m}^{-2} \text{ s}^{-1}$ as in (Falge et al., 2001)), PAR is measured photosynthetic active radiation ($\mu\text{mol quantum m}^{-2} \text{ s}^{-1}$), GPP_{max} is gross primary productivity at its optimum. Due to low coverage of the PAR range in a single measurement campaign, data from multiple campaigns were pooled according to dates, vegetation, and air temperature.

265 **2.4.4 ~~NECB~~ Net ecosystem carbon balance calculations**

270 The NEE is the sum of R_{eco} and GPP values, calculated by applying the hourly monitored soil temperature ~~(-5 cm)~~ and PAR data to the models developed per campaign. Extrapolated values at times between two adjacent models are weighted averages of the estimates from these two models, where the weights are temporal distances of the extrapolated time spots to both of the measurements. To account for the influence from plant biomass on the CO_2 fluxes, linear relationships between grass height and model parameters ($R_{eco,Tref}$, GPP_{max} , and α) were developed. Models developed for the campaign before harvesting were

275 then corrected using the slopes of the linear regressions as the models after the harvest to be applied in the extrapolation. The loss of biomass was therefore accounted according to lowered grass height, different from the studies where model parameters are to zero after harvest (e.g. Beetz et al. 2013). Unrealistic parameters after correction were discarded, and instead adopted from parameters from campaigns with low grass height at the same plot. The annual CO₂ fluxes were thus summing of the hourly R_{eco}, GPP and NEE values. The atmospheric sign convention was used for the calculation of NECB. All C fluxes into
280 the ecosystem where defined as negative (uptake from the atmosphere into the ecosystem), and all C fluxes from the ecosystem to the atmosphere are defined as positive. This also holds for non-atmospheric inputs like manure (negative) and outputs like harvests (positive). Both harvest and manure input are expected to be released as CO₂.

2.4.5 CH₄ and N₂O fluxes

CH₄ and N₂O fluxes per site and measurement campaign were averaged per day. The annual emissions sums for CH₄ where
285 were estimated by linear interpolation between the single measurement dates. Global Warming Potential (GWP) of 34 t CO₂-eq and 298 t CO₂-eq per ton for CH₄ and N₂O-was used according to IPCC standards (Myhre et al., 2013). to calculate the yearly GHG balance.

2.4.6 Uncertainties

The estimation of total uncertainties of the yearly budget should include multiple sources of error, where both model error and
290 uncertainty from extrapolations in time are the most important (Beetz et al., 2013). Therefore, we included these two sources of error and combined them into a total uncertainty in three steps. First, we calculated the model error, which would cover the uncertainties from replications (between the three frames) and the random errors from the measurements, the environmental conditions at the time, and the parameter estimation of R_{eco} and GPP. Standard errors (SE) of the prediction were calculated for each measurement campaign / pooled dataset as the SEs of the midday of the campaign dates. The hourly SEs were then
295 extrapolated linearly between modeled campaigns. Total model error of the annual NEE was therefore calculated following the law of error propagation as the square root of the sum of squared SEs. Second, we attribute the uncertainty from extrapolation to the variations from selecting different gap-filling strategies, since other approaches of annual NEE estimation including different R_{eco} and GPP models would result in different values (Karki et al., 2019).. To quantify this uncertainty, six

R_{eco} models and four GPP models were select from Karki et al. (2019)) and fitted with annual data (Appendix Table A1). The

300 models were evaluated following the thresholds of performance indicators in Hoffmann et al. (2015). Fitted parameters of R_{eco} and GPP models that were performed above the ‘satisfactory’ rating was were accepted and calculated into used to gap-filled NEEs. Based on all the annual NEEs per site and year, standard deviations from the means were considered as the extrapolation uncertainty. In the year 2018, the control site of farm D did not yield any satisfactory R_{eco} model. The uncertainty was thus calculated as the average of all sites.

305 Finally, we calculated the total uncertainties per site and year following the law of error propagation with the uncertainties from the previous steps.

2.5 Statistics

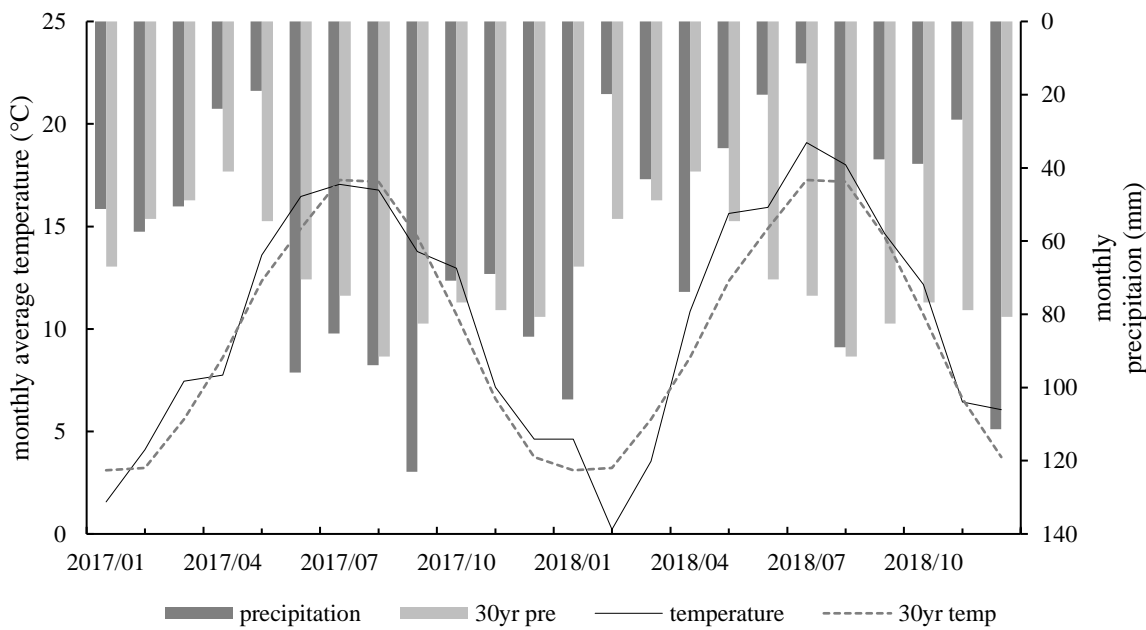
The effect of the treatment on gap-filled annual R_{eco} and GPP, the resulting NEE, the C-export data, the NECB, and the measured CH_4 , N_2O exchanges were tested by fitting linear mixed-effects models, with farm location as a random effect.

310 Effectiveness of the random term was tested using the likelihood ratio test method. Significance of the fixed terms was tested via Satterthwaite's degrees of freedom method. General linear regression was used instead when the mixed effect model gives singular fit. The treatment effect was further tested using campaign-wise R_{eco} data. Measured R_{eco} fluxes from SSI and Control were calculated into daily averages and paired per date. The data pairs were grouped based on the GWT differences between SSI and control of the dates. Differences between treatments were then analyzed by linear regression of the R_{eco} flux pairs 315 without interception and testing the null hypothesis ‘slope of the regression equals to 1’. All statistical analyses were computed using R version 3.5.3 (Team, 2019) using packages lme4 (Bates et al., 2014), lmerTest (Kuznetsova et al., 2017), sjstats (Lüdecke, 2019), and car (Fox and Weisberg, 2018).

3 Results

320 3.1 Weather conditions

Mean annual air temperature was 10.3 °C for 2017 and 10.7 °C for 2018, which were higher than the 30-year average of 10.1 °C. The growing season (April–September) in 2017 was slightly cooler with 14.3 °C than the average of 2018 at 14.6 °C, while the temperature during the growing season in 2018 was 1.1 °C warmer than average. Precipitation was slightly higher for 2017 840–951 mm compared to the 30-year average of 840 mm (K~~MNMN~~I). There was a small period of drought in May and June, 325 ending in the last week of June ([See see](#) Fig.3). In contrast, 2018 was a dry year with average precipitation of 546–611 mm (range of 2 sites in Friesland). The year is characterized by a period of extreme drought in the summer, from June to the beginning of August, and precipitation lower than average in the fall and winter.



330 **Figure 3** Monthly average air temperature at weather station Leeuwarden (18 to 30 km distance from research sites), and the 30-year average. Sum precipitation at weather station Leeuwarden, and the 30-year average.

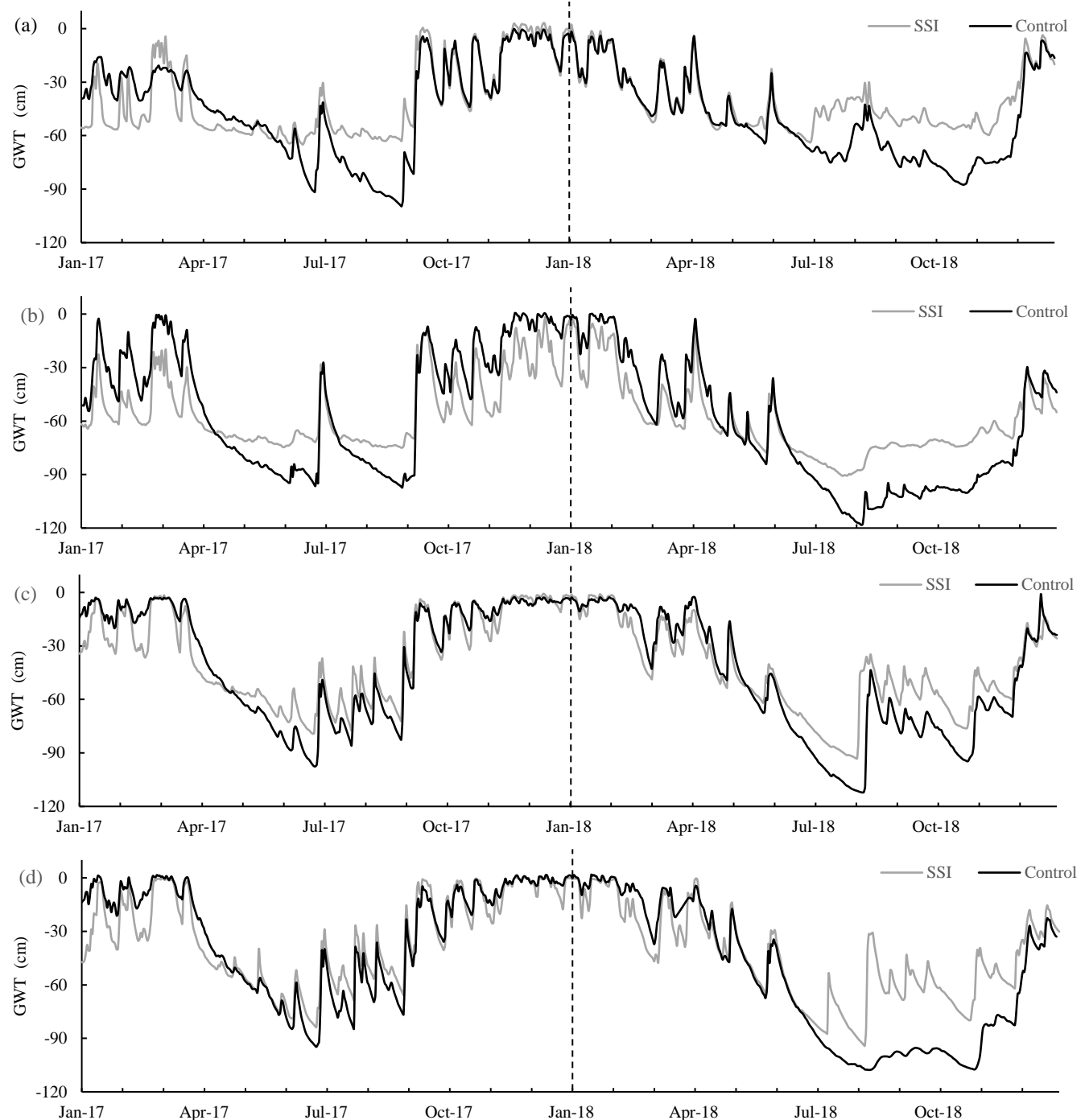


Figure 4 Groundwater table (GWT, from soil surface) during the measuring period per farm (letter), per graph SSI (measured 1.5 m from the irrigation pipe) and control.

3.2 Groundwater table (GWT)

Deploying SSI systems affected ~~the~~ GWT dynamics during the two years for all farms (Fig. 4). However, there was a large variation in effect-size between years and locations. The effect of SSI can be divided into two types of periods. Periods with drainage (decreased GWT), in the wet periods, coincided with the autumn (in 2017) and winter period (2017 and 2018).

340 Irrigation (increased GWT) periods, where the SSI leads to a higher water table than control, occurred during spring and summer when the GWT dipped below the ditch water level. In 2017, the effectiveness differed per farm. For locations A and B, GWT was more stable in summer around the -60 and -70 for SSI compared to the control, while locations C and D the GWT fluctuated more like in the control fields. During the dry summer of 2018, in contrast, all locations showed a strong effect of irrigation, especially after the dry period in the beginning of august. In this period the water table recovered quickly
345 while the control lagged behind.

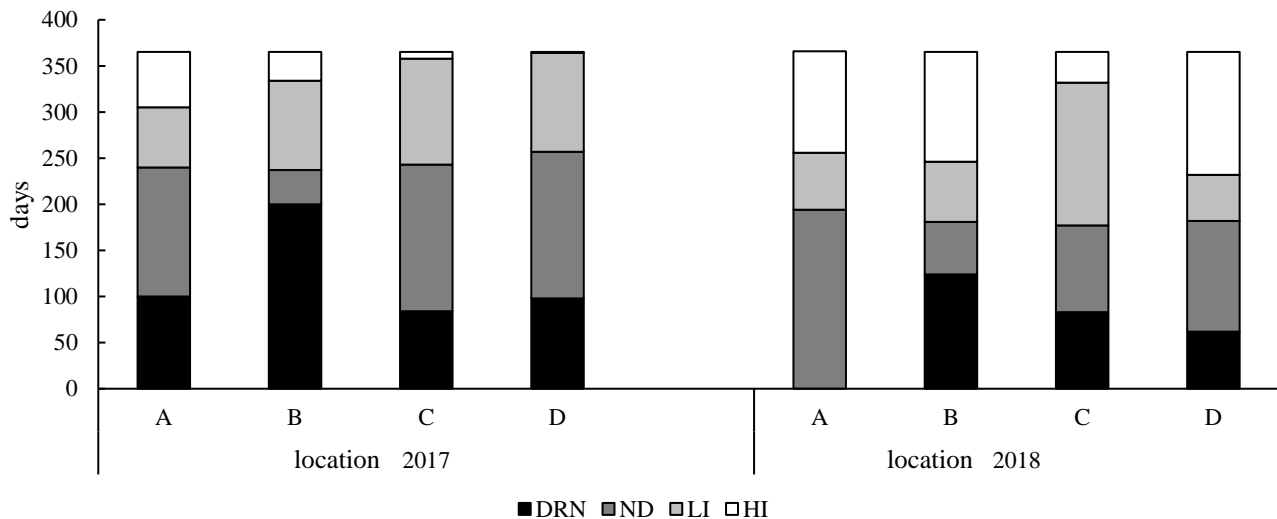


Figure 5 Days with effective drainage/ irrigation for the four locations. drainage (DRN, <-5 cm), no difference (ND, -5 ~ 5 cm), low to intermediate irrigation (LI, 5 ~ 20 cm) and high irrigation (HI, > 20 cm) 1.5 m from the ~~irrigation~~-SSI pipe.

350 Although there was hardly any difference in annual average GWT between control and SSI (~~< 5 cm~~; Table 2), drainage and irrigation effects could be observed when dividing the calendar year into seasons. The effective days of the SSI are summarized in Fig. 5 according to four categories, based on practical definitions of drainage and irrigation: drainage (DRN, <-5 cm), no difference (ND, -5 ~ 5 cm), low to intermediate irrigation (LI, 5 ~ 20 cm) and high irrigation (HI, > 20 cm). These categories

355 classes are also used in the statistical analysis of R_{eco} measurements (see 3.7 Seasonal R_{eco}). In 2017 there were 17 days more without any GWT difference than in 2018. There was a much stronger irrigation effect in the dry year of 2018, with 61 more irrigated days comparing to 2017, and the number of irrigation days was constantly similar to, or higher than the number of drainage days, except for site B in 2017 which had a long period showing a drainage effect.

Table 2:Average Groundwater table (belowcm from soilgroundthe surface level-) groundwater table-during the measuring period per farm. Summer groundwater table ranges from April till October. Measured 1.5 meter from the irrigation-SSI pipe.

Location	Treatment	Average 2017	Summer 2017	Average 2018	Summer 2018
A	SSI	-43	-52	-51	-48
	Control	-40	-63	-41	-59
B	SSI	-47	-64	-67	-71
	Control	-53	-73	-61	-83
C	SSI	-35	-54	-51	-56
	Control	-34	-61	-45	-67
D	SSI	-31	-51	-59	-56
	Control	-32	-56	-45	-77

360

3.3 Measured R_{eco}

Figure. 6 compares the measured R_{eco} fluxes with the corresponding GWT measurements, which could give an indication for the effectiveness of the GWT differences. ~~The division between t~~~~The groups~~~~classes~~ whereas based on the GWT differences between the SSI and control sites on the measurement days (the same ~~groups~~~~classes~~ used in Fig. 5). There was a slightly 365 higher R_{eco} for SSI during drainage periods when GWT was lower (DRN), which compensates for the lower R_{eco} during summer. For moments where there was no GWT difference (ND) and those showing moderate irrigation (LI), there was no effect of SSI on R_{eco} . However, when the GWT of the SSI was more than 20 cm higher than the control (HI), the emissions of the control were significantly higher than SSI ($p < 0.01$), indicating an effect of the irrigation. However, this effect of the raised GWT was small, even though in some cases the GWT was raised more than 60 cm. According to Fig. 5, in 2017, the 370 majority of the days were dominated by drainage (increasing R_{eco}), or by no difference or small irrigation resulting in no effect on the R_{eco} . However, ~~the moments periods~~~~periods~~ with increased irrigation (Fig. 5), when there was a reduced R_{eco} effect of SSI, were sparse compared to the other dominating periods.

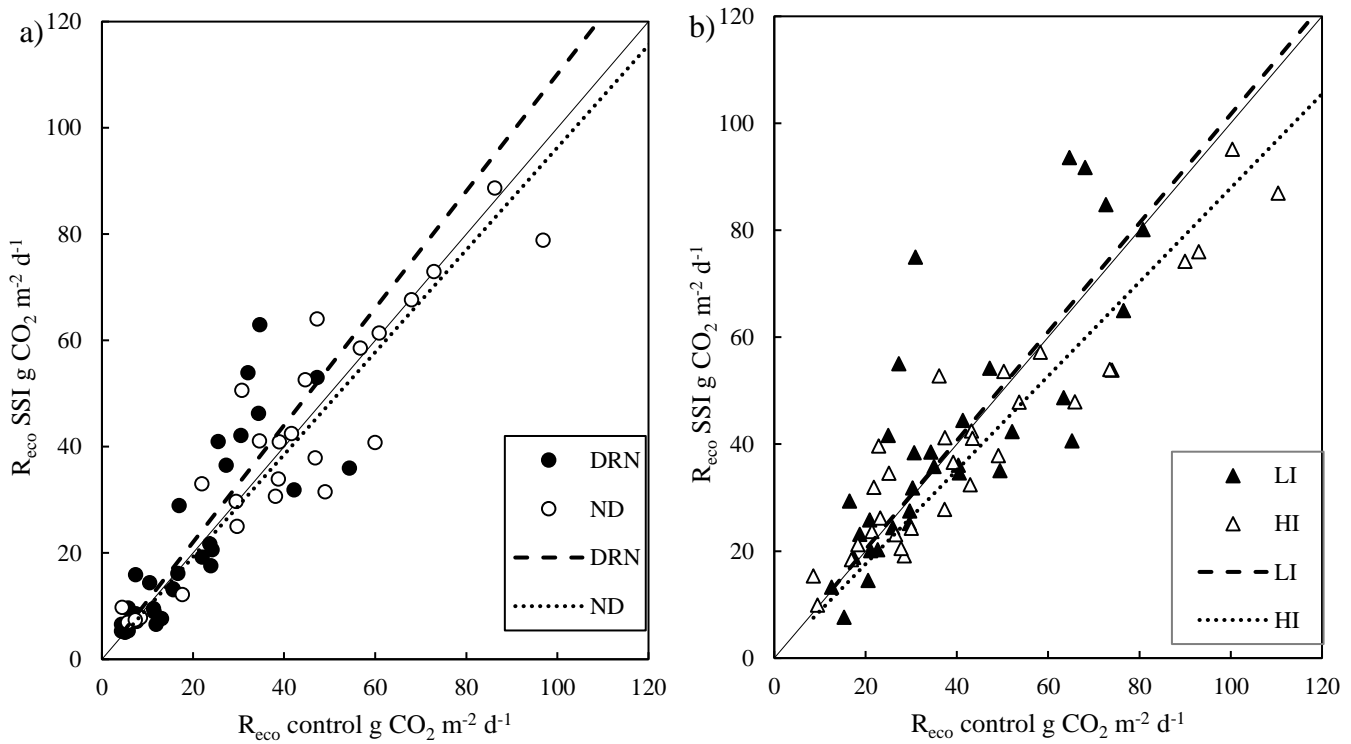


Figure 6 Measured fluxes for ecosystem respiration (R_{eco}), one-to-one comparison in which daily averages where used. a) Values divided into two groups: where the ground water table was lower due to the effect of drainage (DRN), and where there was a limited difference (ND). b) Values divided into two groups with irrigation effects, moderate infiltration with more than 5–20 cm difference (LI) and high infiltration (HI) with more than 20 cm difference between SSI and Control. Black filled line is the 1:1 line.

3.4 Annual carbon fluxes

3.4.1 Gross primary production (GPP)

GPP was high for all locations in both years, showing a clear seasonal pattern with the highest uptake at the start of the summer (Fig. 7). GPP was 30% lower in the dry year 2018 ($p < 0.001$) compared to 2017 (see Table 2) and differed between locations (random effect $p = 0.006$). There was, however, no treatment effect on GPP ($p = 0.3101$). Average GPP values for all SSI and control plots were -88.3 ± 7.5 and -89.2 ± 13 t CO₂ ha⁻¹ yr⁻¹ for 2017, -71.7 ± 6.6 and -65.7 ± 4.9 t CO₂ ha⁻¹ yr⁻¹ for 2018, respectively.

3.4.2 Ecosystem respiration (R_{eco})

R_{eco} was generally high for all the farms measured during the two years, with the average R_{eco} of 128.4±4.6 t CO₂ ha⁻¹ yr⁻¹ for 385 2017 being significantly higher than 100.8±11 t CO₂ ha⁻¹ yr⁻¹ for 2018 (p < 0.001) (Table 2). Different seasonal patterns were also observed between the two years, where in 2017 R_{eco} peaked in June and July, while in 2018 the highest R_{eco} was found in May (Fig. 7, Appendix B). However, no effect of SSI on R_{eco} was found (p = 0.6191), with average R_{eco} values for all SSI and control plots as 128.7±9.2 and 126.7±9.5 t CO₂ ha⁻¹ yr⁻¹ in 2017, 102.1±14.1 and 99.6±13.5 t CO₂ ha⁻¹ yr⁻¹ in 2018.

3.4.3 Net ecosystem exchange (NEE)

390 All locations functioned as large C sources during the measurement period. The average annual NEE of all sites amounted to 39.7±11 and 31.8±8.4 t CO₂ ha⁻¹ yr⁻¹ in 2017 and 2018, respectively. The overall explanatory power of year, treatment and location was low, with no yearly difference between 2017 and 2018 (p = 0.1813), or any treatment effect of SSI (p = 0.9805). The average NEE values for all SSI and control plots are 40.4±11.9 and 37.5±16.1 t CO₂ ha⁻¹ yr⁻¹ in 2017, 30.4±15.6 and 34±14.5 t CO₂ ha⁻¹ yr⁻¹ in 2018, respectively.~~or~~

395 3.4.4 C-export (yield)

C-exports (i.e. yields) differed between years without treatment effect of SSI (p = 0.691). Following the drought in 2018, C export (13.8±0.6 t CO₂ ha⁻¹ yr⁻¹) was significantly lower (p < 0.001) than in 2017 (18.0±1.4 t CO₂ ha⁻¹ yr⁻¹). These values corresponded to dry matter yields of 9.4±0.6 t DM ha⁻¹ yr⁻¹ in 2018 and 12.6±1.1 t DM ha⁻¹ yr⁻¹ in 2017. The year-effect differed per location (random effect p < 0.001). We found a solid relationship between C-export and GPP (p < 0.001, r² = 400 0.942; linear-mixed modeling).

3.4.5 Net ecosystem carbon balance (NECB)

All sites are large carbon sources, without an effect of SSI (p = 0.9446) which was consistent for all farms (Table 3). However, there was a significant difference between the two years, with higher carbon emission rates in 2017 amounting to 49.6±11 t CO₂ eq. ha⁻¹ yr⁻¹ on average, compared with 36.9±7.6 t CO₂ eq. ha⁻¹ yr⁻¹ for 2018 (p=0.0277).

405 **3.5 Methane exchange**

The total exchange of CH₄ was very low during both years with no effect from the SSI ($p=0.1147$) or difference between years ($p=0.1253$). During most periods, the locations functioned as a sink of CH₄. The annual fluxes were -0.01 ± 0.01 t CO₂ eq. ha⁻¹ yr⁻¹ (-0.25 kg CH₄ ha⁻¹ yr⁻¹) for 2017 and -0.06 ± 0.05 t CO₂ eq. ha⁻¹ yr⁻¹ (-1.8 kg CH₄ ha⁻¹ yr⁻¹) for 2018 (Table 4). Such exchange did not play a significant part in the total GHG emissions (comparable to less than 0.4% of the annual NECB).

410 **3.6 Nitrous oxide exchange**

There was no treatment effect ($p=0.5640$) or inter-annual difference ($p=0.4414$) detected. The highest average emissions were measured on the SSI plot of location D, with 5.78 ± 5.9 mg N₂O. m⁻² d⁻¹ for 2017 and 10.7 ± 17.4 mg N₂O. m⁻² d⁻¹ for 2018. The highest peak was measured on the frame closest to the irrigation-SSI pipe in August for SSI of location D, showing 55 ± 15 mg N₂O m⁻² d⁻¹. The peaks observed were erratic and did not correspond to fertilization management with slurry before 415 measurement campaigns.

Table 3 Overview of all processes contributing to the carbon balance calculated for both years. Ecosystems respiration (R_{eco}), gross primary production (GPP), net ecosystems exchange (NEE, sum of GPP and R_{eco}), C-exports (harvest), C-manure (carbon addition from manure application), and net ecosystem carbon balance (NECB, sum of all fluxes) for subsoil irrigation (SSI) and control plots at farm locations A-D. The range of R_{eco} , GPP and NEE represent the combination of model error and extrapolation uncertainties following the law of error propagation.

			Carbon exchange					NECB
Year	Location	treatment	R_{eco} t CO ₂ ha ⁻¹ yr ⁻¹	GPP t CO ₂ ha ⁻¹ yr ⁻¹	NEE t CO ₂ ha ⁻¹ yr ⁻¹	C-export t CO ₂ ha ⁻¹ yr ⁻¹	C-manure t CO ₂ ha ⁻¹ yr ⁻¹	CO ₂ t CO ₂ ha ⁻¹ yr ⁻¹
2017	A	SSI	<u>125.9</u> <u>123.1</u> \pm 3.4	<u>-88.8</u> <u>88.9</u> \pm 2.7	<u>37.1</u> <u>34.2</u> \pm 4.4	16.6 <u>±0.4</u>	-6.9 <u>±0.1</u>	46.8 <u>±4.4</u>
		Control	<u>134.8</u> <u>133.7</u> \pm 6.5	<u>-81.5</u> <u>81.3</u> \pm 7.9	<u>53.3</u> <u>52.4</u> \pm 10.2	19.3 <u>±0.7</u>	-6.9 <u>±0.1</u>	65.7 <u>±10.2</u>
	B	SSI	<u>125.2</u> <u>125</u> \pm 5.8	<u>-97.8</u> <u>98.5</u> \pm 3	<u>27.4</u> <u>26.5</u> \pm 6.5	15.3 <u>±1.1</u>	-5.3 <u>±0.1</u>	37.4 <u>±6.6</u>
		Control	<u>123.4</u> <u>123.2</u> \pm 5.8	<u>-92.2</u> <u>92.6</u> \pm 2.9	<u>31.2</u> <u>30.6</u> \pm 6.5	15.5 <u>±0.0</u>	-5.3 <u>±0.1</u>	41.4 <u>±6.5</u>
	C	SSI	<u>132.5</u> <u>132.1</u> \pm 4.6	<u>-87.9</u> <u>87.7</u> \pm 5.7	<u>44.6</u> <u>44.5</u> \pm 7.4	22.1 <u>±0.2</u>	-10.9 <u>±0.2</u>	55.8 <u>±7.4</u>
		Control	<u>122.7</u> <u>122.3</u> \pm 3.2	<u>100.1</u> <u>100</u> \pm 8.3	<u>22.6</u> <u>22.3</u> \pm 8.9	23.3 <u>±0.9</u>	-10.9 <u>±0.2</u>	35 <u>±8.9</u>
	D	SSI	<u>134.6</u> <u>134.5</u> \pm 4.2	<u>-78.6</u> <u>78.6</u> \pm 2.8	<u>56</u> <u>56</u> \pm 5	15.7 <u>±1.4</u>	-9.3 <u>±0.2</u>	62.4 <u>±5.2</u>
		Control	<u>127.9</u> <u>127.9</u> \pm 2	<u>-82.7</u> <u>82.9</u> \pm 5.3	<u>45.2</u> <u>44.9</u> \pm 5.6	16.3 <u>±0.6</u>	-9.3 <u>±0.2</u>	52.2 <u>±5.6</u>
2018	A	SSI	<u>98</u> <u>98.3</u> \pm 6.5	<u>-74.9</u> <u>74.7</u> \pm 2.5	<u>23.1</u> <u>23.6</u> \pm 7	14 <u>±0.0</u>	-7.4 <u>±0.1</u>	29.7 <u>±7</u>
		Control	<u>101.1</u> <u>101.3</u> \pm 5.5	<u>-69.3</u> <u>68.9</u> \pm 3.1	<u>31.9</u> <u>32.4</u> \pm 6.4	14 <u>±0.0</u>	-7.4 <u>±0.1</u>	38.5 <u>±6.4</u>
	B	SSI	<u>118.1</u> <u>117.5</u> \pm 10.1	<u>-73.8</u> <u>73.4</u> \pm 3.4	<u>44.3</u> <u>44.2</u> \pm 10.7	13.8 <u>±0.6</u>	-9.3 <u>±0.2</u>	48.8 <u>±10.7</u>
		Control	<u>111.5</u> <u>111.4</u> \pm 10.5	<u>-64.6</u> <u>64.5</u> \pm 2.8	<u>46.9</u> <u>46.9</u> \pm 10.9	12.2 <u>±1.2</u>	-9.3 <u>±0.2</u>	49.8 <u>±11</u>
	C	SSI	<u>109.2</u> <u>109.6</u> \pm 5.8	<u>-83</u> <u>82.4</u> \pm 4.6	<u>26.2</u> <u>27.3</u> \pm 7.4	15.7 <u>±1.0</u>	-9.3 <u>±0.2</u>	32.6 <u>±7.5</u>
		Control						

		Control	<u>99.2</u> 99.2 ^{99.2} ±1.3	<u>-74.2-</u> 73.7 ^{-74.2-} ±0.6	<u>25</u> 25.5 ^{25.5} ±1.5	<u>15.8</u> 15.8 ^{15.8} ±0.4	<u>-9.3</u> -9.3 ^{-9.3} ±0.2	<u>31.5</u> 31.5 ^{31.5} ±1.6
D	SSI		<u>82.9</u> 82.9 ^{82.9} ±4.5	<u>-56-</u> 56.1 ⁻⁵⁶⁻ ±2.2	<u>26.9</u> 26.8 ^{26.8} ±5	<u>13.4</u> 13.4 ^{13.4} ±0.23	<u>-9.3</u> -9.3 ^{-9.3} ±0.2	<u>31</u> 31 ³¹ ±5
		Control	<u>86.5</u> 86.6 ^{86.6} ±6.3	<u>-55.9-</u> 55.5 ^{-55.9-} ±2.4	<u>30.6</u> 31.1 ^{31.1} ±7	<u>12</u> 12 ¹² ±0.32	<u>-9.3</u> -9.3 ^{-9.3} ±0.2	<u>33.3</u> 33.3 ^{33.3} ±7

425 **Table 4** The average measured CH₄ and N₂O emissions subsoil irrigation (SSI) and controls for the four locations (A-D) for both years in mg m⁻² d⁻¹. The total CH₄ balance in CO₂ equivalents, using radiative forcing factors of 34 for CH₄ according to IPCC standards (Myhre et al., 2013). The ranges of CH₄ and N₂O represent the standard deviation (SD) of the measured fluxes.

			GHG fluxes		Balance
Year	Location	treatment	CH ₄ mg CH ₄ m ⁻² d ⁻¹	N ₂ O mg N ₂ O m ⁻² d ⁻¹	CH ₄ t CO ₂ eq. ha ⁻¹ yr ⁻¹
2017	A	SSI	-0.44±0.5	0.02±0.7	-0.01
		Control	-0.54±0.9	1.46±1.8	-0.05
	B	SSI	-0.43±0.4	3.81±3.3	-0.04
		Control	-0.27±0.9	2.30±4.9	-0.02
	C	SSI	-0.43±1.0	2.48±1.5	-0.03
		Control	-0.40±0.5	2.56±2.0	0.01
2018	A	SSI	-0.50±0.8	5.78±5.9	0.01
		Control	0.72±2.7	4.81±2.3	0.06
	B	SSI	-0.39±0.7	0.15±0.8	-0.05
		Control	-0.67±1.2	0.80±0.9	-0.12
	C	SSI	-0.40±0.3	2.08±3.7	-0.04
		Control	-0.30±0.9	4.88±3.9	0.00
	D	SSI	-0.73±0.9	3.27±3.0	-0.11
		Control	-0.66±0.9	4.46±3.7	-0.07
		Control	-0.91±0.6	10.7±17.4	-0.09
		Control	-0.14±0.8	2.69±2.2	0.02

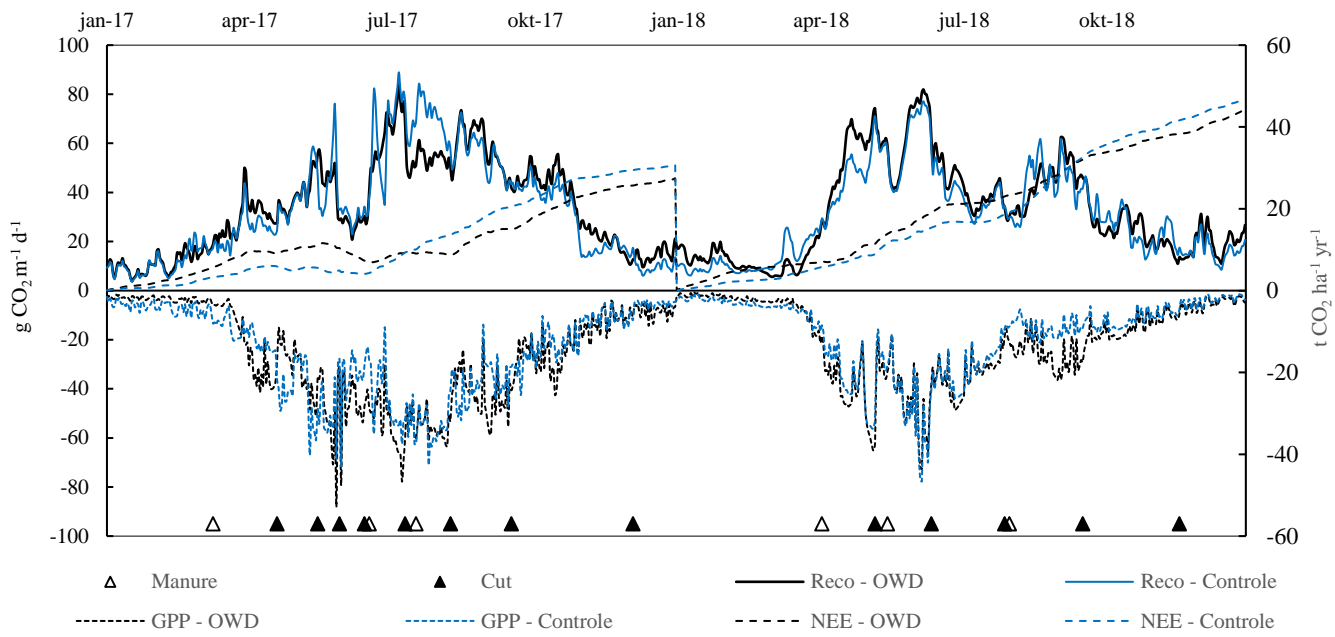


Figure 7 R_{eco} and GPP for location B in $\text{g CO}_2 \text{ m}^{-2} \text{ d}^{-1}$ on the primary y-axis, for control and SSI. Accumulative NEE in $\text{t CO}_2 \text{ ha}^{-1} \text{ yr}^{-1}$, for control and subsoil irrigation (SSI), every year starting at 0.

435 **4 Discussion**

In this experimental research we found effects of subsoil irrigation (SSI) on water table dynamics without changing carbon dynamics profoundly. For both years, SSI had a clear irrigation effect during summer, increasing the averages of GWT during summer period by 6–18 cm at the four farms. During winter, there was a moderate but consistent drainage effect, reducing the average GWT in the wet/winter period by 1–20 cm. Mean annual GWT was little affected by SSI. Despite the irrigation effects and higher water levels in summer, there was no effect of SSI on R_{eco} , GPP and NEE on neither of the two years total GHG balances remained high ($62 \text{ t CO}_2 \text{ eq. ha}^{-1} \text{ yr}^{-1}$ on average of all sites and years with an uncertainty of $3\text{--}16 \text{ t CO}_2 \text{ ha}^{-1} \text{ yr}^{-1}$). We found no evidence for a reduction of CO_2 emissions, nor for higher yield improvements, on an annual base by implementing SSI.

4.1 SSI does not reduce annual R_{eco}

445 We identified 3three conditions that can explain the limited effect of SSI on carbon fluxes most prominent peat decomposition. Firstly, the uppermost 30-40 cm remain drained in both treatments throughout large parts of the year (220-255 days) facilitating increased CO_2 fluxes. Secondly, gas exchange from lower layers (60 cm and below) was presumably low due to moisture levels close to saturation that limit diffusion of CO_2 and O_2 effectively. Thirdly, the deliberate increase in drainage in the SSI treatment frustrate the irrigation effect on GWT. As a consequence, mean annual GWT was similar for both treatments.

450 Based on the direct comparison using measured R_{eco} fluxes (Fig. 6), we found a modest 5–10% reduction in R_{eco} only when GWT differences were larger than 20 cm. When the irrigation effect was smaller, no effect on the R_{eco} was found. An earlier study on intensively managed peat pastures in the Netherlands on the role of GWT also showed small effects of higher summer GWT on annual R_{eco} and NEE despite substantial differences in soil volume changes/soil subsidence (Dirks et al., 2000). Similarly, a 4-year study (Schrier-Uijl et al., 2014) found little differences in NEE estimates despite substantial large variations 455 in summer GWT and soil moisture contents.

Our findings contradict the general assumption that a higher GWT leads to lower CO_2 emissions, which is often found in near natural peatlands with the presence of peat-forming vegetation. However, most studies discuss the effect of annual average GWT, instead of seasonal changes in GWT. It is generally assumed that higher GWT (mean annual or actual) -leads to lower 460 CO_2 emissions according to laboratory data (Moore and Dalva, 1993) Moore and Dalva, 1993 and correlations between annual CO_2 fluxes and mean annual GWT (Wilson et al., 2016; Tiemeyer et al., 2020). In addition However, there are also studies that did not find an effect of GWT on CO_2 emissions during the growing season (Lafleur et al., 2005; Nieven et al., 2005; Parmentier et al., 2009). This lack of effect is explained by the fact that there is only a small variation difference in soil moisture values above the GWT between SSI and Control sites. A large number of studies report The lower CO_2 emissions 465 reported with when water levels were structurally elevated GWT are often, concomitant with substantial differences in vegetation/land use that are adapted to the higher GWT following higher water levels (Beetz et al., 2013; Schrier-Uijl et al., 2014; Wilson et al., 2016), which could confound the effects of GWT change. In our study, SSI seems to have an effect of a similar magnitude trending towards higher emissions during periods with lower GWT at the SSI sites.

470 The ~~small effect sizes~~small treatment effect on measured R_{eco} (Fig. 6) in our study can most probably be explained by differences in peat oxidation rates along the soil profile. Some other studies suggest that the top 30–40 cm ~~layer~~of the peat profile plays an important role in C turnover rates in drained peatlands, due to more readily decomposable C sources and higher temperatures (Moore and Dalva, 1993; Lafleur et al., 2005; Karki et al., 2016; Säurich et al., 2019). This soil layer was, however, not affected by higher summer GWTs in our study. ~~SSI even reduced the number of days (24-27 days) that the top 30-40 cm remained saturated, mostly in the wet season. Moreover, the topsoil layer was even exposed to oxygen for longer periods due to extra drainage during wet seasons. As the infiltrating water will affect the soil moisture content of these layers, it is even expected that this content will approach the optimum for C mineralization more often at the locations where SSI is applied. Moreover,~~
475 ~~Säurich et al. (2019) speculated that the highest CO₂ production in the top 10 cm is reached when GWTs are approximately 40 cm below the surface (Silvola et al., 1996). As the infiltrating water will affect the soil moisture content of these layers, it is possible that SSI could even facilitate rather than mitigate summer emissions by approaching the optimum for C mineralization more often.~~
480

In contrast to surface irrigation, where the topsoil is replenished with moisture, the SSI effect is limited to deeper parts of the peat soils, at -60–100 cm depth. However, the role of this deeper layer as a prominent C source for emissions to the atmosphere 485 is ~~only supposed to remain~~ limited. ~~Its potency to act as a C source is reduced~~CO₂ production and export from deeper layers is prevented by lower temperatures, limited O₂ intrusion, and the fact that water content of this layer is already close to saturation frustrating gas diffusion (Berglund and Berglund, 2011; Taggart et al., 2012; Säurich et al., 2019). This layer shows low levels of stronger electron acceptors such as O₂ and nitrate used for the microbial oxidation of organic compounds, and of labile organic matter (Fontaine et al., 2007; Leifeld et al., 2012). Visually, the layers at our sites deeper than 60 cm ~~are~~were 490 less decomposed (yellow-brown with plant macrofossils still visible) compared to the highly degraded peat in the uppermost 40 cm.

In addition, lower In our case, although CO₂ production in deeper peat layers could be lower due to that are saturated after SSI induced due to the higher water level GWT elevation, this reduction may be compensated by the increased CO₂ production 495 in the top 20–40 cm due to the higher moisture levels resulting from elevated water levels. The dry year of 2018 with very low GWT as low as -120 cm in the control sites (and thus an expected maximized effect of SSI) provides additional evidence that SSI contributes little if any to the mitigation of CO₂ emission from drained peatlands. Such understanding of the processes of CO₂ emissions in relation to soil profiles, along with the assumption from the Dutch soil-carbon-water model that the average 500 lowest summer GWT (i.e. GLG ‘gemiddeld laagste grondwaterstanden’) is the major control of CO₂ emissions, is currently under investigation (STOWA, 2020)

4.2 SSI effects on CH₄ and N₂O emissions

The magnitudes of measured CH₄ and N₂O fluxes are substantially lower than CO₂ fluxes, which would thus lead to negligible contributions to the total GHG emissions in our case. Looking directly at the measured fluxes, no SSI effect was detected for neither CH₄ or N₂O. Findings of this experiment agree with the generally accepted idea that intensively drained 505 peatlands have low levels of CH₄ emissions, and often these systems even function as a small CH₄ sink (Couwenberg et al., 2011; Couwenberg and Fritz, 2012; Tiemeyer et al., 2016; Maljanen et al., 2010). Drainage ditches, in contrast, emitted methane CH₄ at high rates (Kosten et al., 2018; Lovelock et al., 2019). The SSI site in farm D showed the highest N₂O emissions with 10.7±17.4 mg N₂O m⁻² d⁻¹ for 2017. In the current study the average of all measured N₂O emission fluxes 510 was 3.3 mg N₂O m⁻² d⁻¹ (12 kg N₂O ha⁻¹ yr⁻¹), which falling within the range of annual N₂O emissions from drained peatlands in Northern Europe (4–18 kg N₂O ha⁻¹) (Leahy et al., 2004; Maljanen et al., 2010; Schrier-Uijl et al., 2014; Kandel et al., 2018). Fertilization, temperature and water table fluctuations play major roles in the total N₂O emission (Regina et al., 1999; Van Beek et al., 2011; Poyda et al., 2016). No distinct peaks were measured after application of fertilizer, and fertilizer was applied on all locations on the same day, so missing peak fluxes would not influence the comparison. The mechanisms of N₂O production and consumption in organic soils are, however, complex and there is high temporal and spatial variability 515 as influenced by site conditions and management (Leppelt et al., 2014; Taghizadeh-Toosi et al., 2019). It is well studied that periods with frost and thawing result in high N₂O emissions (Koponen and Martikainen, 2004). In this study, the low

measurement frequency in both years does not allow annual estimations of N₂O with enough representation of peak N₂O emission. However, SSI effect still cannot be expected according to the direct comparison of measured fluxes. annual N₂O emissions may have been underestimated by linear interpolation missing potential N₂O emissions peaks in late winter and 520 spring. Because of the low measurement interval for both years The low measurement interval in both years in the winter period, there is a high chance of an underestimation of the N₂O emission, which makes it hardlimits this study testing the effects of SSI on N₂O emissions extensively. However, this would not influence our conclusion on the absent of SSI treatment effect., although this would not result in noticeable changes on the total GHG emissions. It is well studied that periods with frost and thawing result in high N₂O emissions (Koponen and Martikainen, 2004).

525 4.3 Reasonably high NEE

In contrast to the expected function of the SSI technique based on land subsidence data, no effect has been found on either promoting the yield/GPP nor reduction on NEE and other GHG emissions. Our NEE estimates from averaging all sites and years at 35.8 (22.6 – 56.0) t CO₂ ha⁻¹ yr⁻¹ has exceeded is at the higher end of the ranges reported for drained temperate peatlands (Wilson et al. 2016) (Wilson et al., 2016) 2, where Tiemeyer et al. (2020) reported 30.4 (5.1 – 40.3) t CO₂ ha⁻¹ yr⁻¹ for the German 530 drained organic soils in Germany. In a Dutch case study authors found a NECB of 20.1 t CO₂ ha⁻¹ yr⁻¹ average over the years 2005-2008 (Schrier Uijl et al. 2014) (Schrier-Uijl et al., 2014) 2, and Veenendaal et al. (2007) reported 4.9 t CO₂ ha⁻¹ yr⁻¹ in an earlier analysis at an intensively managed Dutch peat meadow measured with eddy covariance. Looking into Comparing GPP and R_{eco} estimates with earlier reports we find that individually, on the one hand, the GPP of the sites was higher than values found by Tiemeyer et al. (2016) for productive and drained peatlands (-70 ± 18 t CO₂ ha⁻¹ yr⁻¹) especially in the year 2017 (- 535 88.7±7.2 t CO₂ ha⁻¹ yr⁻¹), and falls back to the range in 2018 (-69.0±8.9 t CO₂ ha⁻¹ yr⁻¹) due to the drought induced decline of CO₂ uptake (Fu et al., 2020). This could be simply explained by the high productivity of the sites, where Higher GPP estimates seems reasonable give the high the C-export in 2017 (on average 18.0 t CO₂ ha⁻¹) that was substantially larger than the 8.5 t CO₂ ha⁻¹ reported by Tiemeyer et al. (2016) for grassland on organic soils. On the other hand, the R_{eco} values of the sites (128.4±4.6 and 100.8±11 t CO₂ ha⁻¹ yr⁻¹ in 2017 and 2018, respectively) are also -at the higher end of the range (97 ± 33 t CO₂ 540 ha⁻¹ yr⁻¹ in Tiemeyer et al. (2016)). Extrapolation bias was excluded as a possible reason for this high CO₂ emission, since

testing of different R_{eco} modeling approaches (including different model selection, data clustering procedure and removal of raw data outliers) did not yield substantially different R_{eco} values. Järveoja et al. (2020) ~~discovered~~ ~~reported~~ in a boreal natural peatland strong diel patterns of R_{eco} with emission peaks at both midnight and midday. The authors show that daily carbon fluxes were overestimated, which could lead to overestimation of daily fluxes when models ~~are~~ ~~were~~ developed ~~with~~ 545
~~data collected around the peaks~~ including peak emission. In case a ~~Although this process the same~~ similar pattern of R_{eco} applies to ~~is not clear for~~ temperate productive highly productive and drained peatlands systems the flux measurements with opaque chambers to estimate R_{eco} would need to be spread more evenly during day (and ideally throughout the night) In our case, the flux measurements were unevenly distributed and concentrated around midday, which may have led to overestimation of R_{eco} and, therefore, NEE overestimation to avoid overestimation. representativeness of the campaign could be a reason for 550
~~the high R_{eco} estimates~~. Besides the general methodological ~~speculations~~ limitations of the close-chamber method, there are also a number of biochemical reasons for mechanisms that may explain the high emissions found here. Abiotic conditions that favor high CO_2 emissions were present, with high temperatures for both years and non-limiting moisture conditions for 2017. Research from Pohl et al. (2015) found in a drained peatland a high impact of dynamic soil organic carbon (SOC) and N stocks in the aerobic zone on CO_2 fluxes. In our case, the peat soils contained a high amount of C, especially in the upper 20 cm layer. 555
This layer was also aerobic for long periods during the experiment, thus promoting high rates of C formation sequestration and decomposition. transformation processes in the plant-soil system. In conclusion, NEE estimates in the current study are high owing to systemic overestimation of R_{eco} and conditions promoting high soil CO_2 production and release.

4.4 Uncertainties

GHG emissions on peat grasslands are highly variable (Tiemeyer et al., 2016) given the uncertainties from the wide ranges of 560 land use and management activities (Renou-Wilson et al., 2016) and gap filling techniques (Huth et al., 2017). In this study, besides the model errors inherent in the model development process, uncertainties from gap-filling techniques in terms of data-pooling strategies and model selections were also considered. Campaign-wise fitting of R_{eco} and GPP models can best represent the original data sets, while pooling data for a longer period can provide better model fitness and less bias toward single measurements (Huth et al., 2017; Poyda et al., 2017). However, in this study, different responses of vegetation and soil

565 processes to drought, especially to the extreme drought in 2018, caused data points that could not be ~~represented explained~~ by the classic models, resulting in the generally poor performances of annual models. For this reason, we reported the annual budgets with campaign-wise gap-filled NEE values. The uncertainties of NEE estimates from model differences were on average 14 tons and up to 25 tons of CO₂. Nevertheless, no SSI effect was found considering NEE estimates from annual models. The model differences quantified here were in good agreements with other model tests (Görres et al., 2014; Karki et al., 2019) and match the magnitude of NEE uncertainties calculated with other methods (e.g. the 23–30 tons CO₂ variances reported by (Schrier-Uijl et al., 2014) using eddy co-variance techniques). Additionally, CO₂ fluxes and annual budgets derived from eddy co-variance approach in 2019 at location ‘A’ support findings of the present study (Van den Berg and Kruijt, 2020). The eddy co-variance revealed virtual identical flux patterns for both control and SSI field despite drastic differences in summer GWT surpassing 80 cm at the height of the vegetation period.

575 4.5 ~~Costs and benefits of the SSI~~The effects of SSI on land use

The intensity of land use (intensity and timing of drainage and fertilization, plant species composition, mowing and grazing regimes) influence is a major driver of the carbon turnover in grassland’s ability to accumulate or lose C (Renou-Wilson et al., 2016; Smith, 2014; Ward et al., 2016). SSI facilitates earlier fertilization compared to management under current drainage systems SSI can by increasing increasing the load-bearing capacity of the field surface for fertilizing equipment. - We expect nutrient accumulation to continue that can lead to high CO₂ losses accelerated by nitrogen or phosphorus (Tiemeyer et al., 2016; Säurich et al., 2019) Tiemeyer et al., 2016, Säurich et al., 2019 facilitating earlier fertilization compared to management under current drainage systems. This can also cause increased leaching of water due to earlier drainage in a wet spring. However, the general land use intensity will not change with the use of SSI. It was expected that C-export via crop yields due to extra drainage could increase in a wet autumn. However, we did not find any indication for an increase in land-use intensity or yield as a result of SSI. However, the general In summary, land-use intensity will not change with the use of SSI remain high in SSI treatments without substantial changes to carbon sequestrating vegetation (e.g. (Couwenberg et al., 2011; Schrier-Uijl et al., 2014; Tiemeyer et al., 2020) Couwenberg et al., 2011; Schrier Uijl et al., 2014; Tiemeyer et al., 2020

2020), tillage (Smith, 2014) or potential nutrient accumulation (Pohl et al., 2015; Vroom et al., 2020) Pohl et al., 2015:

Vroom et al., 2020).

590 The implementation of SSI may further inflict high costs on land users. Next to investing in 1800 to 2500 m of extra drainage pipes per hectare maintenance costs rise. Drain pipe inspection, cleaning and maintenance cost range between 0.30 to 0.90 € per m with an incurrence interval of 3-6 years depending on abiotic conditions (Klaas Kooistra pers. communication). SSI inflict practical challenges in all catchments where ditcher water levels are difficult to control and where water needs to pumped in during summer. Groundwater extraction has been suggested as an alternative which will further increase direct costs 595 (pumping infrastructure, fuel) and indirect costs including land-subsidence following groundwater extraction (Herrera-García et al., 2021). A large rolle out of SSI seems costly, impractical and holds only few benefits for land use on peatlands.

The use of SSI is considered impractical for use in most regions outside of the Netherlands due to the high investment costs for irrigation SSI pipes and the intensive water infrastructure needed for controlling the water level. In addition, irrigation 600 SSI pipes will increase the water demand in summer for these agricultural fields. Both land use intensity and an increase in yield are related to an increase in CO₂ emissions on drained peat (Couwenberg, 2011; Beetz et al., 2013). The land use history of our sites favors high CO₂ emission: tillage (cultivators, sod renewal, and some plowing), cumulative fertilization and well maintained drainage (Provincie Fryslân, 2015).

5 Main conclusions

605 The implementation of SSI technique with the current design does not lead to a reduction of GHG emissions from drained peat meadows, even though there was a clear increase in GWT during summer (especially in the dry year of 2018). We therefore conclude that the current use of SSI with the aim to raise the water table to -60 cm is ineffective as a mitigation measure to sufficiently lower peat oxidation rates and, therefore, also soil subsidence. Most likely, the largest part of the peat oxidation takes place in the top 40 cm of the soil, which stays above the GWT with the use of SSI remained drained. This layer is still

610 exposed to higher temperatures, sufficient moisture, oxygen and alternative electron acceptors such as nitrate, and nutrient input. We expect that SSI may only be effective when the GWT can be raised permanently to water tablelevels close to the soil-surface.

615 **Data availability.** The data are available on request from the corresponding author, (S.T.J. Weideveld).

CRediT authorship contribution statement:

SW: Investigation, Data curation, Writing – original draft, Visualization, Methodology. WL: Investigation, Data curation, Writing – original draft, Visualization. MB: Data curation, Writing – original draft, Visualization. LL: Writing - review & editing, Supervision. CZCF: Conceptualization, Methodology, Data curation, Writing - original draft, Supervision

620 **Acknowledgements**

We would like to thank all technical staff, students and others who helped in the field and in the laboratory, as well as the land owners who granted access to the measurement sites. We acknowledge Peter Cruisen and Roy Peters for their assistance in practical work and analyses. Weier Liu is supported by the China Scholarship Council.

625 Grants: WL is supported by the China Scholarship Council. MB was supported by the NWO-Peatwise grant. CF received funding from ERA-NET Climate Smart Agriculture.

Appendix A Annual models

Table A1. Model selected for annual-model gap-filling approach of year budgets (adopted from Karki et al. 2019), as a measure of extrapolation ~~uncertainties~~uncertainties.

Model	Structure	Description
R _{eco}	1 $Reco_{T_{ref}} * e^{E_0 * \left(\frac{1}{T_{ref} - T_0} - \frac{1}{T - T_0} \right)}$	Arrhenius function as used for the campaign-wise model fit. Parameters follow descriptions in Material and Methods.
	2 $(Reco_{T_{ref}} + (\alpha * GH)) * e^{E_0 * \left(\frac{1}{T_{ref} - T_0} - \frac{1}{T - T_0} \right)}$	Model 1 adding <i>GH</i> (grass height) as a vegetation factor. α is a scaling parameter of <i>GH</i> .
	3 $Reco_{T_{ref}} * e^{E_0 * \left(\frac{1}{T_{ref} - T_0} - \frac{1}{T - T_0} \right)} + (\alpha * GH)$	Different form of vegetation included Model 1.
	4 $R_0 * e^{bT}$	Exponential function. R_0 is respiration at 0 °C, b is a temperature sensitivity parameter.
	5 $(R_0 + (\alpha * GH)) * e^{bT}$	Model 4 with vegetation included.
	6 $R_0 + (b * T) + (\alpha * GH)$	Linear function.
GPP	1 $\frac{\alpha * PAR * GPP_{max}}{GPP_{max} + \alpha * PAR}$	Michaelis-Menten light response curve as used for the campaign-wise model fitting.
	2 $\frac{\alpha * PAR * GPP_{max} * GH}{GPP_{max} * GH + \alpha * PAR} * FT$	Model 1 with vegetation and air temperature included. FT is a temperature dependent function of photosynthesis set to 0 below - 2 °C and 1 above 10 °C and

			with an exponential increase between - 2 and 10 °C.
3	$\frac{GPP_{max} * PAR}{\kappa + PAR} * \left(\frac{GH}{GH + a} \right)$		Another form of the Michaelis-Menten light response curve with a vegetation term included. a is a model-specific parameter.
4	$\frac{GPP_{max} * PAR}{\kappa + PAR} * \left(\frac{GH}{GH + a} \right) * FT$		Model 3 with air temperature included.

Appendix B—Soil type deeryption

Table B1 Soil characteristics of the research sites in Frisian peat meadows. Average per soil type, gravimetric soil moisture content taken August 2017, Dry bulk density, Organic matter content, and elemental Carbon content.

Farm	Treatment	Soil type	Depth	Soil	Bulk	Organic	Carbon
				moisture %	density g DW/cm ³	matter g Org/L	content g C/L
A	SSI	Mineral	0-35	38.1	0.99	122.6	52.3
		Peat	35-60	77.1	0.23	144.0	77.1
		Peat	60-80	82.1	0.14	130.4	67.9
	Control	Mineral	0-40	37.6	0.93	130.1	53.6
		Peat	40-60	59.2	0.24	156.0	82.9
		Peat	60-80	85.3	0.16	153.8	98.1
	B	SSI	0-20	51.0	0.44	270.3	107.6
		Peat	20-60	79.3	0.19	168.9	76.6
		Peat	60-80	88.4	0.12	118.3	59.9
	Control	Peat	0-20	50.1	0.49	273.4	138.3
		Peat	20-60	77.7	0.17	140.6	72.0
		Peat	60-80	86.5	0.13	122.0	66.9
C	SSI	Mineral	0-30	36.0	0.71	127.9	58.2
		Schalter	30-40	79.2	0.19	176.9	87.5
		Peat	40-60	82.2	0.18	128.5	64.2
		Peat	60-80	87.5	0.11	132.9	81.4
	Control	Mineral	0-30	38.0	0.75	141.7	59.2
		Schalter	30-40	78.7	0.19	176.9	92.4
		Peat	40-60	84.3	0.12	116.3	59.9
		Peat	60-80	89.2	0.10	133.6	71.5
D	SSI	Mineral	0-30	37.7	0.85	154.5	73.7
		Schalter	30-40	63.9	0.30	266.5	85.2
		Peat	40-60	84.3	0.19	137.0	73.1
		Peat	60-80	80.2	0.14	129.6	54.6
	Control	Mineral	0-25	32.9	0.82	140.7	73.3
		Schalter	25-35	70.0	0.27	172.6	85.9
		Peat	35-60	84.1	0.15	141.9	82.7
		Peat	60-80	81.9	0.11	108.5	69.5

Appendix C-B Reco ,GPP and NEE

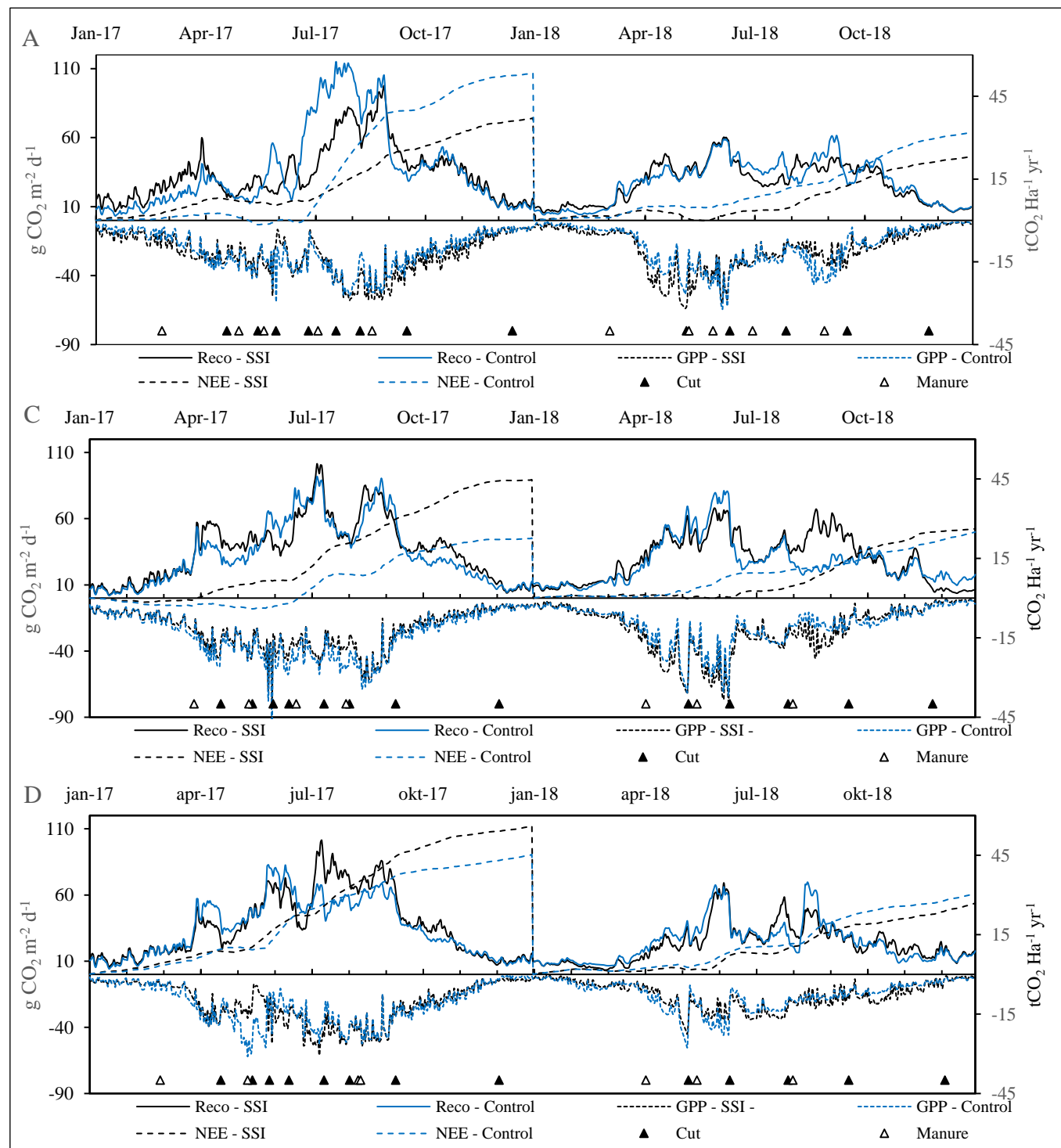


Figure BC1 Daily Reco and GPP for location in $\text{g CO}_2 \text{ m}^{-2} \text{ d}^{-1}$ on the primary y-axis, for control and SSI for locations A,C and D. Accumulative NEE in $\text{tCO}_2 \text{ Ha}^{-1} \text{ yr}^{-1}$, for control and SSI, every year starting at 0.

Appendix D-C CH₄ exchange

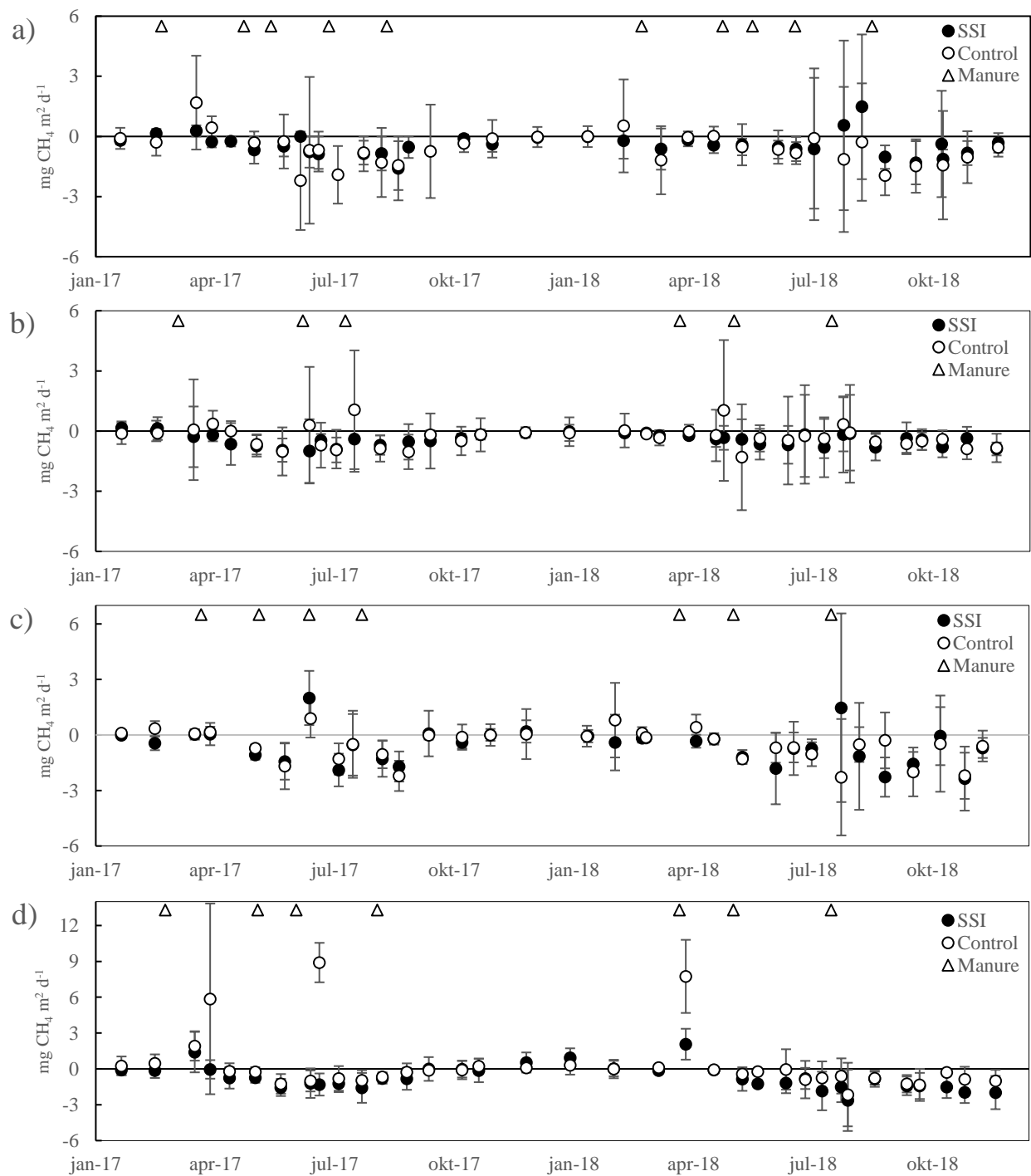


Figure D-C1 CH₄ exchange throughout 2017 and 2018 in mg CH₄ m⁻² d⁻¹

Appendix E-D N₂O exchange

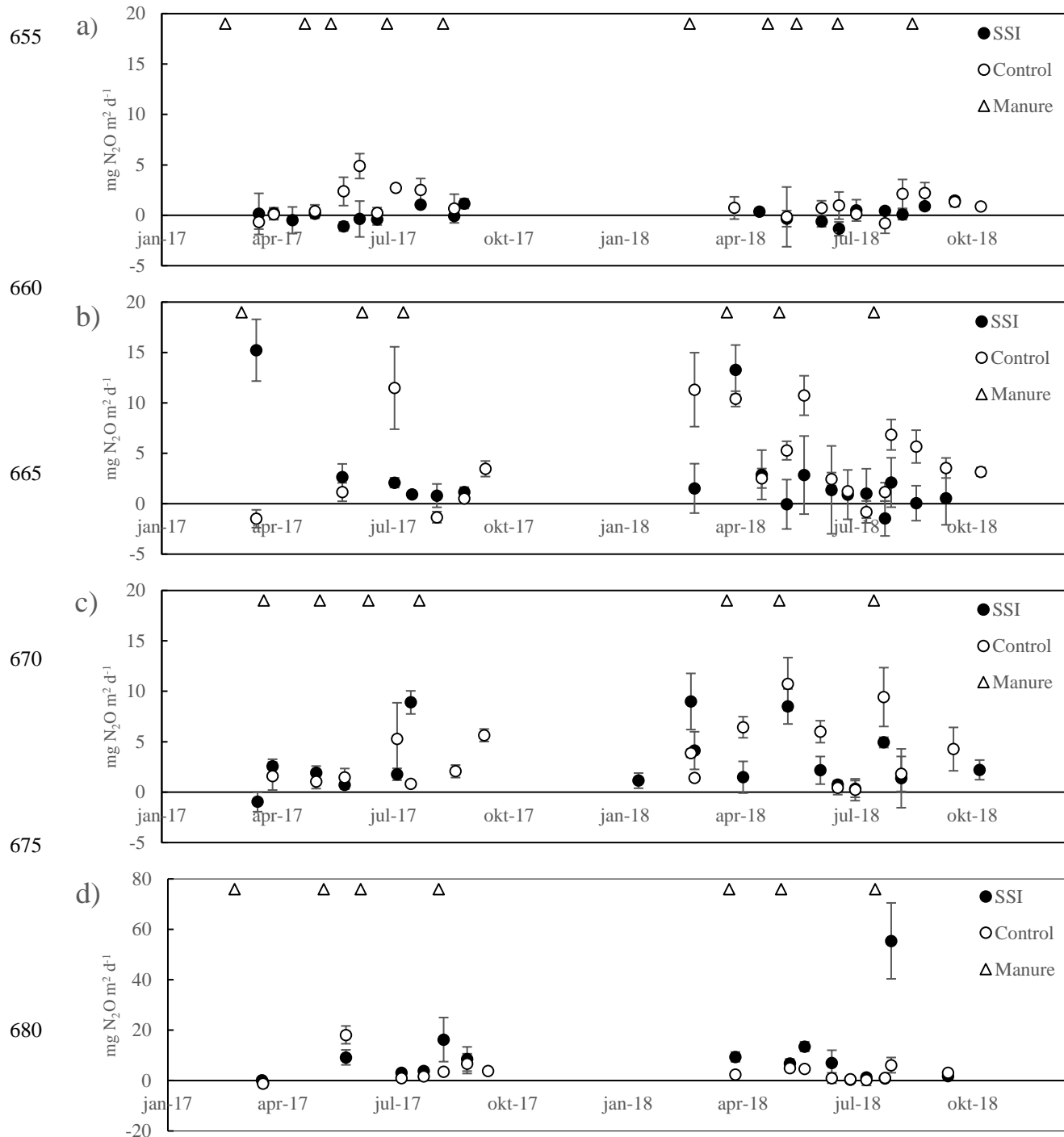


Figure E-D1 N₂O exchange throughout 2017 and 2018 in mg N₂O m⁻² d⁻¹.

References

685 Almeida, R. M., Nóbrega, G. N., Junger, P. C., Figueiredo, A. V., Andrade, A. S., de Moura, C. G., Tonetta, D., Oliveira Jr, E. S., Araújo, F., and Rust, F.: High primary production contrasts with intense carbon emission in a eutrophic tropical reservoir, *Frontiers in microbiology*, 7, 717, 2016.

690 Arets, E. J. M. M., Van Der Kolk, J., Hengeveld, G. M., Lesschen, J. P., Kramer, H., Kuikman, P., and Schelhaas, N.: Greenhouse gas reporting for the LULUCFsector in the Netherlands: methodological background, update 2020, *Statutory Research Tasks Unit for Nature & the Environment*2352-2739, 2020.

695 Bates, D., Mächler, M., Bolker, B., and Walker, S.: Fitting linear mixed-effects models using lme4, *arXiv preprint arXiv:1406.5823*, 2014.

700 Beetz, S., Liebersbach, H., Glatzel, S., Jurasinski, G., Buczko, U., and Höper, H.: Effects of land use intensity on the full greenhouse gas balance in an Atlantic peat bog, *Biogeosciences*, 10, 1067-1082, 2013.

705 Berglund, Ö., and Berglund, K.: Influence of water table level and soil properties on emissions of greenhouse gases from cultivated peat soil, *Soil Biology and Biochemistry*, 43, 923-931, 2011.

710 Brouns, K., Eikelboom, T., Jansen, P. C., Janssen, R., Kwakernaak, C., van den Akker, J. J., and Verhoeven, J. T.: Spatial analysis of soil subsidence in peat meadow areas in Friesland in relation to land and water management, climate change, and adaptation, *Environmental management*, 55, 360-372, 2015.

Couwenberg, J.: Greenhouse gas emissions from managed peat soils: is the IPCC reporting guidance realistic?, *Mires & Peat*, 8, 2011.

715 Couwenberg, J., Thiele, A., Tanneberger, F., Augustin, J., Bärisch, S., Dubovik, D., Liashchynskaya, N., Michaelis, D., Minke, M., and Skuratovich, A.: Assessing greenhouse gas emissions from peatlands using vegetation as a proxy, *Hydrobiologia*, 674, 67-89, 2011.

720 Couwenberg, J., and Fritz, C.: Towards developing IPCC methane 'emission factors' for peatlands (organic soils), *Mires and Peat*, 10, 1-17, 2012.

Dawson, Q., Kechavarzi, C., Leeds-Harrison, P., and Burton, R.: Subsidence and degradation of agricultural peatlands in the Fenlands of Norfolk, UK, *Geoderma*, 154, 181-187, 2010.

725 Dirks, B., Hensen, A., and Goudriaan, J.: Effect of drainage on CO₂ exchange patterns in an intensively managed peat pasture, *Climate Research*, 14, 57-63, 2000.

730 Erkens, G., van der Meulen, M. J., and Middelkoop, H.: Double trouble: subsidence and CO₂ respiration due to 1,000 years of Dutch coastal peatlands cultivation, *Hydrogeology Journal*, 24, 551-568, 2016.

Falge, E., Baldocchi, D., Olson, R., Anthoni, P., Aubinet, M., Bernhofer, C., Burba, G., Ceulemans, R., Clement, R., and Dolman, H.: Gap filling strategies for long term energy flux data sets, *Agricultural and Forest Meteorology*, 107, 71-77, 2001.

735 Fontaine, S., Barot, S., Barré, P., Bdioui, N., Mary, B., and Rumpel, C.: Stability of organic carbon in deep soil layers controlled by fresh carbon supply, *Nature*, 450, 277-280, 2007.

Fox, J., and Weisberg, S.: *An R companion to applied regression*, Sage Publications, 2018.

740 Fu, Z., Ciais, P., Bastos, A., Stoy, P. C., Yang, H., Green, J. K., Wang, B., Yu, K., Huang, Y., and Knohl, A.: Sensitivity of gross primary productivity to climatic drivers during the summer drought of 2018 in Europe, *Philosophical Transactions of the Royal Society B*, 375, 20190747, 2020.

Gorham, E., Lehman, C., Dyke, A., Clymo, D., and Janssens, J.: Long-term carbon sequestration in North American peatlands, *Quaternary Science Reviews*, 58, 77-82, 2012.

745 Görres, C.-M., Kutzbach, L., and Elsgaard, L.: Comparative modeling of annual CO₂ flux of temperate peat soils under permanent grassland management, *Agriculture, ecosystems & environment*, 186, 64-76, 2014.

Hartman, A., Schouwenaars, J., and Moustafa, A.: De kosten voor het waterbeheer in het veenweidegebied van Friesland, *H 2 O*, 45, 25, 2012.

750 Heiri, O., Lotter, A. F., and Lemcke, G.: Loss on ignition as a method for estimating organic and carbonate content in sediments: reproducibility and comparability of results, *Journal of paleolimnology*, 25, 101-110, 2001.

Hendriks, R., Wollewinkel, R., and Van den Akker, J.: Predicting soil subsidence and greenhouse gas emission in peat soils depending on water management with the SWAP-ANIMO model, *Proceedings of the First International Symposium on Carbon in Peatlands*, Wageningen, The Netherlands, 15-18 April 2007, 2007, 583-586.

755 Herbert, E. R., Boon, P., Burgin, A. J., Neubauer, S. C., Franklin, R. B., Ardón, M., Hopfensperger, K. N., Lamers, L. P., and Gell, P.: A global perspective on wetland salinization: ecological consequences of a growing threat to freshwater wetlands, *Ecosphere*, 6, 1-43, 2015.

Herrera-García, G., Ezquerro, P., Tomás, R., Béjar-Pizarro, M., López-Vinielles, J., Rossi, M., Mateos, R. M., Carreón-Freyre, D., Lambert, J., and Teatini, P.: Mapping the global threat of land subsidence, *Science*, 371, 34-36, 2021.

Hiraishi, T., Krug, T., Tanabe, K., Srivastava, N., Baasansuren, J., Fukuda, M., and Troxler, T.: 2013 supplement to the 2006 IPCC guidelines for national greenhouse gas inventories: Wetlands, IPCC, Switzerland, 2014.

760 Hoffmann, M., Jurisch, N., Borraz, E. A., Hagemann, U., Drösler, M., Sommer, M., and Augustin, J.: Automated modeling of ecosystem CO₂ fluxes based on periodic closed chamber measurements: A standardized conceptual and practical approach, *Agricultural and forest meteorology*, 200, 30-45, 2015.

Hoogland, T., Van den Akker, J., and Brus, D.: Modeling the subsidence of peat soils in the Dutch coastal area, *Geoderma*, 171, 92-97, 2012.

740 Hooijer, A., Page, S., Canadell, J., Silvius, M., Kwadijk, J., Wosten, H., and Jauhainen, J.: Current and future CO₂ emissions from drained peatlands in Southeast Asia, *Biogeosciences*, 2010.

Hoving, I., Vereijken, P., van Houwelingen, K., and Pleijter, M.: Hydrologische en landbouwkundige effecten toepassing onderwaterdrains bij dynamisch slootpeilbeheer op veengrond, *Wageningen UR Livestock Research*, 2013.

745 Huth, V., Vaidya, S., Hoffmann, M., Jurisch, N., Günther, A., Gundlach, L., Hagemann, U., Elsgaard, L., and Augustin, J.: Divergent NEE balances from manual-chamber CO₂ fluxes linked to different measurement and gap-filling strategies: A source for uncertainty of estimated terrestrial C sources and sinks?, *Journal of Plant Nutrition and Soil Science*, 180, 302-315, 2017.

Järveoja, J., Nilsson, M. B., Crill, P. M., and Peichl, M.: Bimodal diel pattern in peatland ecosystem respiration rebuts uniform temperature response, *Nature communications*, 11, 1-9, 2020.

750 Joosten, H., and Clarke, D.: Wise use of mires and peatlands: background and principles including a framework for decision-making, *International Mire Conservation Group*, 2002.

Joosten, H.: The Global Peatland CO₂ Picture: peatland status and drainage related emissions in all countries of the world, *The Global Peatland CO₂ Picture: peatland status and drainage related emissions in all countries of the world.*, 2009.

Jurasinski, G., Glatzel, S., Hahn, J., Koch, S., Koch, M., and Koebisch, F.: Turn on, fade out-methane exchange in a coastal fen over a period of six years after rewetting, *EGU General Assembly Conference Abstracts*, 2016.

755 Kabat, P., Fresco, L. O., Stive, M. J., Veerman, C. P., Van Alphen, J. S., Parmet, B. W., Hazeleger, W., and Katsman, C. A.: Dutch coasts in transition, *Nature Geoscience*, 2, 450-452, 2009.

Kandel, T. P., Lærke, P. E., and Elsgaard, L.: Effect of chamber enclosure time on soil respiration flux: A comparison of linear and non-linear flux calculation methods, *Atmospheric environment*, 141, 245-254, 2016.

Kandel, T. P., Laerke, P. E., and Elsgaard, L.: Annual emissions of CO₂, CH₄ and N₂O from a temperate peat bog: Comparison of an undrained and four drained sites under permanent grass and arable crop rotations with cereals and potato, *Agricultural and Forest Meteorology*, 256, 470-481, 2018.

760 Karki, S., Elsgaard, L., Kandel, T. P., and Lærke, P. E.: Carbon balance of rewetted and drained peat soils used for biomass production: a mesocosm study, *Gcb Bioenergy*, 8, 969-980, 2016.

Karki, S., Kandel, T., Elsgaard, L., Labouriau, R., and Lærke, P.: Annual CO₂ fluxes from a cultivated fen with perennial grasses during two initial years of rewetting, *Mires & Peat*, 25, 2019.

765 Koponen, H. T., and Martikainen, P. J.: Soil water content and freezing temperature affect freeze-thaw related N₂O production in organic soil, *Nutrient Cycling in Agroecosystems*, 69, 213-219, 2004.

Kosten, S., Weideveld, S., Stepina, T., and Fritz, C.: Mid-term report: Monitoring Greenhouse gas emissions from ditches in the Netherlands, 2018.

Kuikman, P., van den Akker, J., and de Vries, F.: Emission of N₂O and CO₂ from organic agricultural soils, *Alterra report*, 1035, 2005.

770 Kuznetsova, A., Brockhoff, P. B., and Christensen, R. H. B.: lmerTest package: tests in linear mixed effects models, *Journal of Statistical Software*, 82, 2017.

Lafleur, P., Moore, T. R., Roulet, N. T., and Frolking, S.: Ecosystem respiration in a cool temperate bog depends on peat temperature but not water table, *Ecosystems*, 8, 619-629, 2005.

775 Lamers, L. P., Vile, M. A., Grootjans, A. P., Acreman, M. C., van Diggelen, R., Evans, M. G., Richardson, C. J., Rochefort, L., Kooijman, A. M., and Roelofs, J. G.: Ecological restoration of rich fens in Europe and North America: from trial and error to an evidence-based approach, *Biological Reviews*, 90, 182-203, 2015.

Leahy, P., Kiely, G., and Scanlon, T. M.: Managed grasslands: A greenhouse gas sink or source?, *Geophysical Research Letters*, 31, 2004.

Leifeld, J., Steffens, M., and Galego-Sala, A.: Sensitivity of peatland carbon loss to organic matter quality, *Geophysical Research Letters*, 39, 2012.

780 Leifeld, J., and Menichetti, L.: The underappreciated potential of peatlands in global climate change mitigation strategies, *Nature communications*, 9, 1-7, 2018.

Leppelt, T., Dechow, R., Gebbert, S., Freibauer, A., and Lohila, A.: Nitrous oxide emission budgets and land-use-driven hotspots for organic soils in Europe, *Biogeosciences*, 11, 6595-6612, 2014.

Lloyd, J., and Taylor, J.: On the temperature dependence of soil respiration, *Functional ecology*, 315-323, 1994.

785 Lovelock, C., Evans, C., Barros, N., Prairie, Y., Alm, J., Bastviken, D., Beaulieu, J., Garneau, M., Harby, A., and Harrison, J.: 2019 Refinement to the 2006 IPCC Guidelines for National Greenhouse Gas Inventories, Chapter 7 Wetlands, 2019.

Lüdecke, D.: sjstats: Statistical Functions for Regression Models (Version 0.17.4). doi: 10.5281/zenodo.1284472. 2019.

Maljanen, M., Sigurdsson, B., Guðmundsson, J., Óskarsson, H., Huttunen, J., and Martikainen, P.: Greenhouse gas balances of managed peatlands in the Nordic countries—present knowledge and gaps, *Biogeosciences*, 7, 2711-2738, 2010.

790 Moore, T., and Dalva, M.: The influence of temperature and water table position on carbon dioxide and methane emissions from laboratory columns of peatland soils, *Journal of Soil Science*, 44, 651-664, 1993.

Myhre, G., Shindell, D., Bréon, F., Collins, W., Fuglestvedt, J., Huang, J., Koch, D., Lamarque, J., Lee, D., and Mendoza, B.: Anthropogenic and Natural Radiative Forcing, *Climate Change 2013: The Physical Science Basis. Contribution of Working Group I to the Fifth Assessment Report of the Intergovernmental Panel on Climate Change*, 659–740. Cambridge: Cambridge University Press, 2013.

795 Nieveen, J. P., Campbell, D. I., Schipper, L. A., and Blair, I. J.: Carbon exchange of grazed pasture on a drained peat soil, *Global Change Biology*, 11, 607-618, 2005.

Parmentier, F., Van der Molen, M., De Jeu, R., Hendriks, D., and Dolman, A.: CO₂ fluxes and evaporation on a peatland in the Netherlands appear not affected by water table fluctuations, *Agricultural and forest meteorology*, 149, 1201-1208, 2009.

800 Pohl, M., Hoffmann, M., Hagemann, U., Giebels, M., Albiac Borraz, E., Sommer, M., and Augustin, J.: Dynamic C and N stocks--key factors controlling the C gas exchange of maize in heterogenous peatland, *Biogeosciences*, 12, 2015.

Poyda, A., Reinsch, T., Kluß, C., Loges, R., and Taube, F.: Greenhouse gas emissions from fen soils used for forage production in northern Germany, *Biogeosciences*, 13, 5221-5244, 2016.

Poyda, A., Reinsch, T., Skinner, R. H., Kluß, C., Loges, R., and Taube, F.: Comparing chamber and eddy covariance based net ecosystem CO₂ exchange of fen soils, *Journal of Plant Nutrition and Soil Science*, 180, 252-266, 2017.

805 Querner, E., Jansen, P., Van Den AKKER, J., and Kwakernaak, C.: Analysing water level strategies to reduce soil subsidence in Dutch peat meadows, *Journal of hydrology*, 446, 59-69, 2012.

Regina, K., Silvola, J., and Martikainen, P. J.: Short-term effects of changing water table on N₂O fluxes from peat monoliths from natural and drained boreal peatlands, *Global Change Biology*, 5, 183-189, 1999.

810 Regina, K., Syväsalo, E., Hannukkala, A., and Esala, M.: Fluxes of N₂O from farmed peat soils in Finland, *European Journal of Soil Science*, 55, 591-599, 2004.

Regina, K.: Greenhouse gas emissions of cultivated peatlands and their mitigation, *Suo*, 65, 21-23, 2014.

Renou-Wilson, F., Müller, C., Moser, G., and Wilson, D.: To graze or not to graze? Four years greenhouse gas balances and vegetation composition from a drained and a rewetted organic soil under grassland, *Agriculture, Ecosystems & Environment*, 222, 156-170, 2016.

815 Säurich, A., Tiemeyer, B., Dettmann, U., and Don, A.: How do sand addition, soil moisture and nutrient status influence greenhouse gas fluxes from drained organic soils?, *Soil Biology and Biochemistry*, 135, 71-84, 2019.

Schrier-Uijl, A., Kroon, P., Hendriks, D., Hensen, A., Van Huissteden, J., Berendse, F., and Veenendaal, E.: Agricultural peatlands: towards a greenhouse gas sink-a synthesis of a Dutch landscape study, *Biogeosciences*, 11, 4559, 2014.

Silvola, J., Alm, J., Ahlholm, U., Nykanen, H., and Martikainen, P. J.: CO₂ fluxes from peat in boreal mires under varying temperature and moisture conditions, *Journal of ecology*, 219-228, 1996.

820 Smith, P.: Do grasslands act as a perpetual sink for carbon?, *Global change biology*, 20, 2708-2711, 2014.

Stephens, J. C., Allen Jr, L., and Chen, E.: Organic soil subsidence, *Reviews in Engineering Geology*, 6, 107-122, 1984.

STOWA: Nationaal onderzoeksprogramma broeikasgassen veenweide: Eb en vloed in de polder. In: STOWA Ter info, 2020.

Syvitski, J. P., Kettner, A. J., Overeem, I., Hutton, E. W., Hannon, M. T., Brakenridge, G. R., Day, J., Vörösmarty, C., Saito, Y., and Giosan, L.: Sinking deltas due to human activities, *Nature Geoscience*, 2, 681, 2009.

825 Taggart, M., Heitman, J. L., Shi, W., and Vepraskas, M.: Temperature and Water Content Effects on Carbon Mineralization for Sapric Soil Material, *Wetlands*, 32, 939-944, 2012.

Taghizadeh-Toosi, A., Clough, T., Petersen, S. O., and Elsgaard, L.: Nitrous Oxide Dynamics in Agricultural Peat Soil in Response to Availability of Nitrate, Nitrite, and Iron Sulfides, *Geomicrobiology Journal*, 1-10, 10.1080/01490451.2019.1666192, 2019.

Tanneberger, F., Moen, A., Joosten, H., and Nilsen, N.: The peatland map of Europe, *Mires and Peat*, 19, pp. 1-17, 2017.

830 Team, R. C.: A language and environment for statistical computing. Vienna, Austria: R Foundation for Statistical Computing; 2012, URL <https://www.R-project.org>, 2019.

Tiemeyer, B., Albiac Borraz, E., Augustin, J., Bechtold, M., Beetz, S., Beyer, C., Drösler, M., Ebli, M., Eickenscheidt, T., and Fiedler, S.: High emissions of greenhouse gases from grasslands on peat and other organic soils, *Global change biology*, 22, 4134-4149, 2016.

835 Tiemeyer, B., Freibauer, A., Borraz, E. A., Augustin, J., Bechtold, M., Beetz, S., Beyer, C., Ebli, M., Eickenscheidt, T., and Fiedler, S.: A new methodology for organic soils in national greenhouse gas inventories: Data synthesis, derivation and application, *Ecological Indicators*, 109, 105838, 2020.

Tiggeloven, T., De Moel, H., Winsemius, H. C., Eilander, D., Erkens, G., Gebremedhin, E., Loaiza, A. D., Kuzma, S., Luo, T., and Iceland, C.: Global-scale benefit–cost analysis of coastal flood adaptation to different flood risk drivers using structural measures, *Nat. Hazards Earth Syst. Sci*, 20, 1025-1044, 2020.

840 Van Beek, C., Pleijter, M., and Kuikman, P.: Nitrous oxide emissions from fertilized and unfertilized grasslands on peat soil, *Nutrient cycling in agroecosystems*, 89, 453-461, 2011.

Van den Akker, J., Beuving, J., Hendriks, R., and Wolleswinkel, R.: Maaiveldaling, afbraak en CO₂ emissie van Nederlandse veenweidegebieden, *Leidraad Bodembescherming*, afl, 83, 83, 2007.

845 Van den Akker, J., Kuikman, P., De Vries, F., Hoving, I., Pleijter, M., Hendriks, R., Wolleswinkel, R., Simões, R., and Kwakernaak, C.: Emission of CO₂ from agricultural peat soils in the Netherlands and ways to limit this emission, *Proceedings of the 13th International Peat Congress After Wise Use–The Future of Peatlands*, Vol. 1 Oral Presentations, Tullamore, Ireland, 8–13 june 2008, 2010, 645-648.

Van den Berg, M., and Kruijt, B.: Valitatie effectiviteit van onderwaterdrainage op CO₂ fluxen in Friesland met eddy covariance, 2020.

Van den Born, G., Kragt, F., Henkens, D., Rijken, B., Van Bemmel, B., Van der Sluis, S., Polman, N., Bos, E. J., Kuhlman, T., and Kwakernaak, C.: Dalende bodems, stijgende kosten: mogelijke maatregelen tegen veenbodemdalung in het landelijk en stedelijk gebied: beleidsstudie, Planbureau voor de Leefomgeving, 2016.

Veenendaal, E., Kolle, O., Leffelaar, P., Schrier-Uijl, A., Van Huissteden, J., Van Walsem, J., Möller, F., and Berendse, F.: CO₂ exchange and carbon balance in two grassland sites on eutrophic drained peat soils, 2007.

Vroom, R. J., Temmink, R. J., van Dijk, G., Joosten, H., Lamers, L. P., Smolders, A. J., Krebs, M., Gaudig, G., and Fritz, C.: Nutrient dynamics of Sphagnum farming on rewetted bog grassland in NW Germany, *Science of the Total Environment*, 726, 138470, 2020.

855 Ward, S. E., Smart, S. M., Quirk, H., Tallowin, J. R., Mortimer, S. R., Shiel, R. S., Wilby, A., and Bardgett, R. D.: Legacy effects of grassland management on soil carbon to depth, *Global change biology*, 22, 2929-2938, 2016.

Wilson, D., Blain, D., Couwenberg, J., Evans, C., Murdiyarno, D., Page, S., Renou-Wilson, F., Rieley, J., Sirin, A., and Strack, M.: Greenhouse gas emission factors associated with rewetting of organic soils, *Mires and Peat*, 17, 2016.